

# Effects of short-distance modifications to general relativity in spinning binary systems

Aline Nascimento Lins

*Departamento de Física Teórica e Experimental,  
Universidade Federal do Rio Grande do Norte,  
Av. Sen. Salgado Filho, Natal-RN 59078-970, Brazil*

Riccardo Sturani

*International Institute of Physics, Universidade Federal do Rio Grande do Norte,  
Campus Universitário, Lagoa Nova CP:1613, Natal-RN 59078-970, Brazil\**

We investigate the possibility of testing short distance modifications to General Relativity via higher curvature terms in the fundamental gravity Lagrangian by analysing their impact on observations of spinning astronomical binary systems. By using effective field theory methods applied to the 2-body problem, generic lower bounds on the short-distance scale accompanying high curvature terms can be set. In particular we extend known results by deriving spin-dependent effects in binding energy, radiation emission process, and spin precession equations in binary systems, which are the fundamental ingredients to observe spin-dependent effects in gravitational wave detections from compact binary coalescences and spin precession in double binary pulsars.

Keywords: General Relativity, High-order operators, Effective field theory, Binary systems

## I. INTRODUCTION

The recent Gravitational Wave (GW) detections [1, 2] by the LIGO [3] and Virgo [4] large interferometers have opened a new chapter in the history of physics and astronomy, with countless new investigation which are now made possible. The output of GW detectors is processed via *matched-filtering* [5], which is particularly sensitive to the phase of the GW

---

\*Electronic address: alinelins@fisica.ufrn.br, riccardo@iip.ufrn.br

signals, bearing the imprint of both the astrophysical parameter of the source, like masses and spins, and of the details of the gravitational theory, well in its non-linear regime, ruling the motion of the 2-body system sourcing GWs.

In the present work we admit the possibility that General Relativity (GR) may not be the ultimate theory of gravity but may be completed at *short distances* (UV henceforth) by higher curvature terms. We adopt the framework introduced by [6], i.e. we add *quartic* curvature terms of the type Riemann to the fourth power to the (gauge-fixed) Einstein-Hilbert Lagrangian and compute their lowest order effects, in both the spinning and non-spinning case, to the 2-body dynamics by using the effective field theory methods for gravity pioneered in [7], later applied also to spinning sources [8, 9], also known as Non-Relativistic GR (NRGR).

The introduction of higher curvature terms than in GR introduces new phenomenological constants (with dimensions) parameterising the strength of the GR modifications, playing the role of the UV cutoff of the effective theory.

We consider in this work astronomical observations of *spinning* binary systems, focusing on both detection of GWs from compact binary coalescences and observation of double binary pulsars, which also allows a measure of individual pulsar spin precession.

We extend the work of [6] by systematically computing the linear-in-spin processes in two-body potential and two-body radiation emission derived from the GR-modified model proposed there (from which we find a minor qualitative discrepancy in the radiative sector, see discussion in sec. III A 2). While energy and luminosity functions are necessary ingredients to construct GW-form template to analyse data collected by GW detectors, spin-precession as observed in binary pulsars or by Gravity Probe B [36] can also provide GR precision tests. In view of the application to spinning systems we derive linear-in-spin phenomenological effects by computing the *geodetic precession* of spins in a binary systems within the same GR-modified model, which is also an original contribution of this work.

The paper is organised as follows: in sec. II we summarise the GR UV completion introduced in [6] and briefly review the effective field theory method description of gravity for non-relativistic (i.e for small velocity) spinning systems [9, 10]. In sec. III we present the computation of the effects that higher-curvature terms have for both spinning and non spinning binary systems on the energy and luminosity function which determine the GW-phasing, and on the spin precession in binary systems, the treatment of the spinning case

being the main original part of present work. A discussion of the results and comparisons with current observational limits are presented in sec. IV.

## II. METHOD

Considering a generic parameterisation of possible UV completions of GR, we adopt the effective Lagrangian proposed in [6]

$$\mathcal{S}_{eff} = \frac{1}{16\pi G_N} \int d^4x \sqrt{-g} \left( R - \frac{1}{2} \Gamma^\mu \Gamma_\mu + \frac{\mathcal{C}^2}{\Lambda^6} + \frac{\mathcal{C}\tilde{\mathcal{C}}}{\Lambda_-^6} + \frac{\tilde{\mathcal{C}}^2}{\tilde{\Lambda}^6} \right), \quad (1)$$

with  $R$  the Ricci scalar,  $\Gamma^\mu \equiv g^{\nu\rho} \Gamma_{\nu\rho}^\mu$  enters the gauge fixing term and

$$\begin{aligned} \mathcal{C} &\equiv R_{\alpha\beta\gamma\delta} R^{\alpha\beta\gamma\delta}, \\ \tilde{\mathcal{C}} &\equiv R_{\alpha\beta\gamma\delta} \epsilon^{\alpha\beta\mu\nu} R_{\mu\nu\rho\sigma} g^{\gamma\rho} g^{\delta\sigma}. \end{aligned} \quad (2)$$

Eq. (1) adds to the Einstein-Hilbert Lagrangian terms at *fourth* order of the curvature, where  $\Lambda, \Lambda_-, \tilde{\Lambda}$  are constant with unit of inverse length. Terms quadratic in curvature tensors do not contribute to the equations of motions as they can be written in terms of total derivatives plus terms vanishing on the equations of motion, and cubic terms are forbidden by the causality argument presented in [11].

For non- or mildly-relativistic binary systems it is natural to expand perturbatively the dynamics according to the post-Newtonian (PN) approximation of GR, i.e terms at  $n$ -th PN order are of the type  $G_N^{n-j+1} v^{2j}$ , with  $0 \leq j \leq n$ , the case  $n = j = 0$  corresponding to the leading order (LO) Newtonian potential, being  $v$  the relative velocity of binary components.

The extra terms introduce bulk interactions of quartic and higher orders affecting the equation of motions and the radiation emission (note that to derive the GW phase dynamical evolution one needs both the energy of bound orbits and the luminosity function) for both non-spinning and spinning sources.

Defining  $M \equiv m_1 + m_2$  as the sum of rest masses of binary constituents  $m_{1,2}$ , and introducing for later use the reduced mass  $\mu \equiv m_1 m_2 / M$  and the symmetric mass ratio  $\eta \equiv \mu / M$ , straightforward dimensional argument shows that the quartic interactions introduced above add to the two-body potential terms of the order of  $(GM/r)^3 / (\Lambda r)^6$ , leading to corrections of the order  $2\text{PN} \times 1 / (\Lambda r)^6$ , and analogously for the spin equations of motion, with exception for the parity violating term  $\mathcal{C}\tilde{\mathcal{C}}$  that will be discussed later.

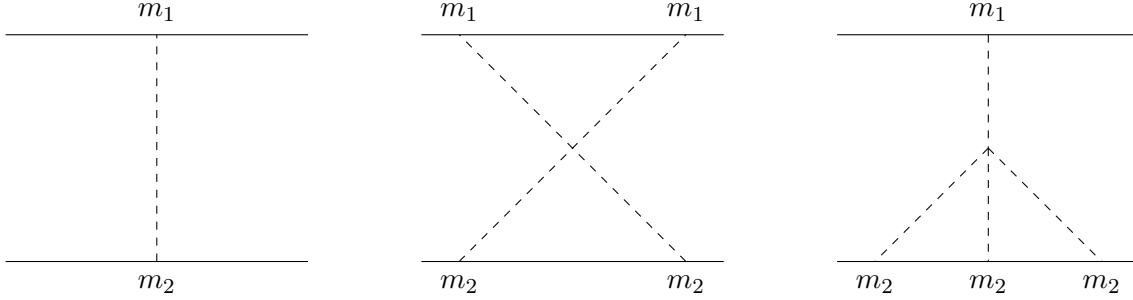


Figure 1: Diagrams representing the Newtonian potential (first on the left) and the leading corrections from the Riemann<sup>4</sup> terms in the fundamental Lagrangian in eq. (1). Last diagram must be supplemented with its mirror image under  $1 \leftrightarrow 2$ .

To make contact with the  $v$  expansion of the PN approximation, we find convenient to express the metric via the Kaluza-Klein (KK) parameterisation [12]

$$g_{\mu\nu} = e^{2\phi/m_{Pl}} \begin{pmatrix} -1 & \frac{A_i}{m_{Pl}} \\ \frac{A_j}{m_{Pl}} & e^{-c_d\phi/m_{Pl}} \left( \delta_{ij} + \frac{\sigma_{ij}}{m_{Pl}} \right) - \frac{A_i A_j}{m_{Pl}^2} \end{pmatrix}, \quad (3)$$

with  $m_{Pl} \equiv (32\pi G_N)^{-1/2}$ ,  $c_d \equiv 2(d-1)/(d-2)$ , where  $d$  is the number of space dimension,  $d = 3$  in the rest of this work, and Latin indices  $i, j \dots$  run over pure space dimensions. The quadratic terms of the gravity bulk Lagrangian, unaffected by the  $\mathcal{C}^2, \mathcal{C}\tilde{\mathcal{C}}, \tilde{\mathcal{C}}^2$  terms, are then given by

$$\mathcal{S}_{eff} = \int d^{d+1}x \sqrt{-\gamma} \left\{ \frac{1}{4} [(\nabla_k \sigma)^2 - 2(\nabla_k \sigma_{ij})^2 - (\dot{\sigma}^2 - 2(\dot{\sigma}_{ij})^2)] - c_d [(\nabla_k \phi)^2 - \dot{\phi}^2] + \left[ \frac{1}{2} F_{ij}^2 + (\nabla_k A_i)^2 - \dot{A}_i^2 \right] \right\}, \quad (4)$$

with  $\sigma \equiv \sigma_{ij} \delta^{ij}$ , where time and space-derivatives have been split to make manifest the scaling in  $v$  of the potential gravitational modes as their derivatives scale differently with  $v$ :  $\frac{d}{dt} \sim v^i \partial_i$ .

The parameterisation in eq. (3) has the advantage that expanding around the Minkowski metric  $\eta_{\mu\nu} \equiv \text{diag}(-1, 1, 1, 1)$  it returns diagonal Feynman propagators for the fields  $\phi, A_i, \sigma_{ij}$

[13, 14]:

$$\left. \begin{aligned} P[\phi, \phi] &= -\frac{1}{8} \\ P[A_i, A_j] &= \frac{\delta_{ij}}{2} \\ P[\sigma_{ij}, \sigma_{kl}] &= -\frac{1}{2} (\delta_{ik}\delta_{jl} + \delta_{il}\delta_{jk} - 2\delta_{ij}\delta_{kl}) \end{aligned} \right\} \times \frac{i}{k^2 - k_0^2 - i\epsilon}, \quad (5)$$

where  $k \equiv |\vec{k}|$  is the modulus of the three-momentum.

## A. Spin-less case

### 1. Two-body potential in GR

The standard coupling to gravity of a spin-less particle of mass  $m_a$  with trajectory  $x_a$  is given by the world-line

$$\mathcal{S}_{pp-wl}|_{\vec{s}=0} = -m_a \int d x_a \tau \supset \frac{m_a}{m_{Pl}} \int_{x_a} dt \left[ -\phi + A_i v_i + \frac{1}{2} \sigma_{ij} v^i v^j + \dots \right], \quad (6)$$

where dots stand for non-linear coupling with gravity fields and higher order in velocity expansion. The lowest order potential is given by the first diagram in fig. 1 <sup>1</sup>

$$V_N = -\frac{m_1 m_2}{8m_{Pl}^2} \int_{\mathbf{k}} \frac{e^{i\vec{k}\cdot\vec{r}}}{k^2} = -\frac{G_N m_1 m_2}{r}, \quad (7)$$

which is the standard Newton potential, obtained by taking the static limit of both the world-line action eq. (6) and of the propagators (5). The additional diagrams in fig. 1 are the LO ones modifying the Newtonian potential due to Riemann<sup>4</sup> terms in eq. (1).

### 2. Radiation emission in GR

The coupling of a binary system to radiative gravitational modes in GR can be computed via the diagrams in fig. 2 [7], i.e. by analysing the emission of a (trace-less)  $\sigma_{ij}$  mode, which gives the following LO effective Lagrangian:

$$\mathcal{L}_{rad-I} = \frac{1}{2} T^{ij} \frac{\sigma_{ij}}{m_{Pl}} \quad (8)$$

$$= \frac{m_1}{2} \left( v_1^i v_1^j - \frac{G_N m_2 r^i r^j}{2r^3} \right) \frac{\sigma_{ij}}{m_{Pl}} + (1 \leftrightarrow 2). \quad (9)$$

<sup>1</sup> We adopt the notation  $\int_{\mathbf{k}} \equiv \int \frac{d^d k}{(2\pi)^d}$  and  $d = 3$  throughout this paper.

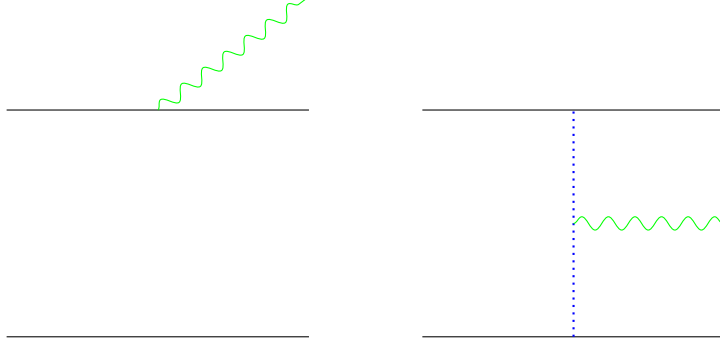


Figure 2: Diagrams describing LO radiative process from a spin-less binary system. The first one must be supplemented by its mirror image under  $1 \leftrightarrow 2$ . Green wavy lines represent radiation, blue dotted line are  $\phi$  longitudinal modes.

By using the (spin-less) Newtonian equation of motion

$$\vec{a}_1|_{\vec{s}_{1,2}=0} = -\frac{G_N m_2 \vec{r}}{r^3}, \quad (10)$$

one can recast eq. (9) into the following standard form

$$\mathcal{L}_{rad-I} = -\frac{1}{2} I^{ij} R_{0i0j}, \quad (11)$$

where  $I^{ij}$  is the radiative electric quadrupole which at LO equals the (trace-less) mass quadrupole  $Q^{ij} = \sum_{a=1}^2 m_a (x_a^i x_a^j - \frac{1}{3} \delta^{ij} x_a^2)$  and  $R_{0i0j}$  is the *electric* part of the Riemann tensor, whose explicit expression at linear order in the metric perturbation reads:

$$m_{Pl} R_{0i0j} \simeq -\frac{1}{2} (\ddot{\sigma}_{ij} - \dot{A}_{i,j} - \dot{A}_{j,i}) + \phi_{,ij} + \frac{\delta_{ij}}{d-2} \ddot{\phi}. \quad (12)$$

More generally, the radiative coupling can be equivalently expressed either in terms of moments of space-space components the energy-momentum tensor like in (8), or in terms of mass and momentum multipole moments like in (11). The derivation of the equivalence is a standard GR-course exercise which uses the conservation of the energy-momentum tensor

$$T^{\mu\nu}_{,\nu} = 0, \quad (13)$$

and we report here the radiative multipolar coupling up to NLO in terms of the electric octupole  $O^{ijk}$  and the magnetic quadrupole  $J^{ij}$ , see app. A for details,

$$L_{rad-GR} = - \int dt \left( \frac{1}{2} I^{ij} \mathcal{E}_{ij} + \frac{1}{6} O^{ijk} \mathcal{E}_{ij,k} - \frac{2}{3} J^{ij} \mathcal{B}_{ij} \right) + \text{higher multipoles}, \quad (14)$$

where  $\mathcal{E}_{ij} \equiv R_{0i0j}$  and  $\mathcal{B}_{ij} \equiv \frac{1}{2}\epsilon_{ikl}R_{0jkl}$  is the magnetic part of the Riemann tensor. From (14) one can derive the standard GR flux formula which is given, writing explicitly only the electric and magnetic quadrupole contributions, by [15]

$$F = G_N \left( \frac{1}{5} \ddot{I}_{ij}^2 + \frac{16}{45} \ddot{J}_{ij}^2 + \dots \right), \quad (15)$$

from which the electric quadrupole contribution gives the LO formula for emission of GWs from circular orbits  $F_{LOcirc} = \frac{32}{5G_N}\eta^2v^{10}$ .

## B. Spin degrees of freedom in GR

Spin degrees of freedom in GR require the introduction of additional degrees of freedom than just position and velocity, embodied by two tetrads:  $e_a^\mu$ , relating the metric into the locally free-falling frame [16, 17]

$$g_{\mu\nu}e_a^\mu e_b^\nu = \eta_{ab}, \quad (16)$$

and  $e_A^\mu$ , co-rotating with the spinning body, and related to the former by a local Lorentz transformation  $e_A^\mu = \Lambda_A^a e_a^\mu$  (we use  $a, b, c, d$  to denote flat space-time Lorentz indices with their capitalised version transforming under the residual Lorentz invariance).

The transport of  $e_A^\mu$  along the world-line of a reference point chosen inside the extended body defines the generalised angular velocity  $\Omega^{\mu\nu}$

$$\frac{de^{A\mu}}{d\tau} \equiv u^\rho e_{;\rho}^{A\mu} = \Omega_\nu^\mu e^{A\nu} \implies \Omega^{\mu\nu} = e_A^\mu \frac{de^{A\nu}}{d\tau} = -\Omega^{\nu\mu}, \quad (17)$$

where  $u^\rho$  is the four-velocity of the object's world-line. Local coordinate, Lorentz and parameterisation invariances require the Lagrangian to be made of invariant contractions of  $\Omega^{\mu\nu}$ ,  $u^\rho$  and eventually of the local curvature tensors, but do not unambiguously fix its form even in the case of flat space-time. However it turns out that if one neglects finite-size effects the variation of any possible Lagrangians w.r.t. to the spinning body local position and tetrad, when expressed in terms of the conjugate momenta  $p^\mu = \frac{\delta\mathcal{L}}{\delta u_\mu}$  and  $S^{\mu\nu} = \frac{\delta\mathcal{L}}{\delta\Omega_{\mu\nu}}$ , gives the *Mathisson-Papapetrou* equations of motion [18–20]:

$$\begin{aligned} \frac{dp^\mu}{d\tau} &= -\frac{1}{2}R_{\mu\nu\rho\sigma}u^\nu S^{\rho\sigma}, \\ \frac{dS^{\mu\nu}}{d\tau} &= p^\mu u^\nu - p^\nu u^\mu. \end{aligned} \quad (18)$$

Since the physical spin variables are related to the conjugate momentum  $S^{\mu\nu}$  rather than to the fundamental tetrad variables, it can be convenient to work with a functional that behaves as an Hamiltonian with respect to the spin, while remaining a Lagrangian with respect to the body position  $x^\mu$ . Such hybrid functional is called a Routhian [21], defined as the Legendre transform of the Lagrangian  $\mathcal{L}$ , which gives the explicit form (valid up to linear order in the spin)

$$\mathcal{R} = m\sqrt{u^2} + \frac{1}{2}\omega_\mu^{ab}S_{ab}u^\mu, \quad (19)$$

being  $\omega_\mu^{ab} \equiv e^{b\nu}e_{\nu;\mu}^a$  the spin connection. One then recovers the Mathisson-Papapetrou equations via

$$\frac{\delta}{\delta x^\mu} \int dt \mathcal{R} = 0, \quad \frac{dS^{ab}}{d\tau} = \{\mathcal{R}, S^{ab}\}, \quad (20)$$

once the following Poisson bracket is taken into account<sup>2</sup>:

$$\{S^{ab}, S^{cd}\} = \eta^{ad}S^{bc} + \eta^{bc}S^{ad} - \eta^{ac}S^{bd} - \eta^{bd}S^{ac}. \quad (21)$$

The anti-symmetric tensor  $S^{\mu\nu}$  (which appears above through its locally flat-frame components  $S^{ab} \equiv S^{\mu\nu}e_\mu^a e_\nu^b$ ) is the generalised, relativistically-covariant spin of the body, however it contains redundant degrees of freedom. The redundancy corresponds to the ambiguity related the choice of a reference world-line inside the body. One can reduce from 6 to the 3 degrees of freedom needed to describe an ordinary spin vector by imposing the *Spin Supplementary Condition* (SSC), which relates the 3-vector  $S^{0i}$  to the physical spin components  $S^i \equiv \frac{1}{2}\varepsilon^{ijk}S_{jk}$ . There is not a unique way to impose such condition, e.g. one can use the *covariant* SSC  $S^{\mu\nu}p_\nu = 0$  condition [16], the *baryonic*  $S^{i0} = \frac{1}{2}S^{ij}u_j$  [22], among others, both of which can be described at LO by

$$S^{i0} = \kappa S^{ij}v_j, \quad (22)$$

with  $\kappa = 1, \frac{1}{2}$ . The requirement of SSC conservation along the world line shifts the momentum of the particle by a quantity *quadratic* in the spin [16], and it will be neglected in this work that is restricted to liner-in-spin effects.

---

<sup>2</sup> Note the difference in sign with respect to eq. (8.25) of [9], where a mostly minus metric signature convention is used.



Being an algebraic constraint, as far as the orbital equation of motions are concerned, the SSC can be imposed by direct replacement of  $S^{i0}$  indifferently at the level of the fundamental Routhian, in the effective potential or in the equations of motion: we will adopt here the second option (substitute into the potential). However when deriving the spin equations of motion the SSC constraint has to be imposed at the level of the equation of motions, i.e. after applying the Poisson bracket in eq. (20).

Note that adopting the covariant SSC, i.e.  $\kappa = 1$  in eq. (22), the Poisson brackets become *non-canonical*: brackets between coordinates and between coordinates and spin do not vanish [16]. Instead of dealing with a non-canonical algebra one can equivalently shift the world-line of each particle according to [17]

$$\vec{x}_{1,2} \rightarrow \vec{x}_{1,2} - \frac{1}{2m_{1,2}} \vec{S}_{1,2} \times \vec{v}_{1,2}, \quad (23)$$

and use a canonical algebra when deriving the equation of motions for coordinates and spin, or equivalently one can adopt the baryonic SSC,  $\kappa = 1/2$  in eq. (22), and use canonical Poisson brackets [17].

The spin-dependent part of the world-line action in terms of the KK parameterisation, for a particle with mass  $m$  and velocity  $v$  at linear order in spin is (for  $d = 3$ )<sup>3</sup> [23]

$$\mathcal{S}_{pp-wl} \supset \frac{1}{m_{Pl}} \int_{x_a} dt \left[ S^{ij} \left( -\frac{1}{4} F_{ij} + \frac{1}{2} \sigma_{ik,j} v_a^k + \phi_{,j} v_{ai} + \frac{1}{4} F_{jk} \sigma_i^k + \frac{1}{2} \sigma_{ik} (\phi_{,j} v_a^k + \phi^{,k} v_{aj}) \right) \right. \\ \left. + S^{0i} \left( -\phi_{,i} + \frac{1}{2} \dot{\sigma}_{ij} v_a^j - \frac{1}{2} \phi_{,j} \sigma_{ij} \right) \right], \quad (24)$$

where all field are understood to be evaluated on the world-line of the source-particle and we displayed only terms that will be needed in the rest of this work.

For power counting spin  $|\vec{S}_a| \sim G_N m_a^2$ , angular momentum  $|\vec{L}| \sim \eta G_N M^2 / v$  hence terms linear in spin, i.e. of the type  $\vec{S} \cdot \vec{L}$  appear at lower order than terms  $\sim \vec{S}^2$  in the PN expansion.

### 1. Spin terms in two-body potential in GR

The lowest order spin contribution to the two body potential in GR occurs at 1.5PN order, i.e.  $v^3$  order with respect to the leading, and is due to the sum of the two processes

---

<sup>3</sup> Note that the point-particle Routhian has the same sign as the potential, hence opposite sign with respect to the Lagrangian.

represented in fig. 3 (and their mirror images under  $1 \leftrightarrow 2$ ).

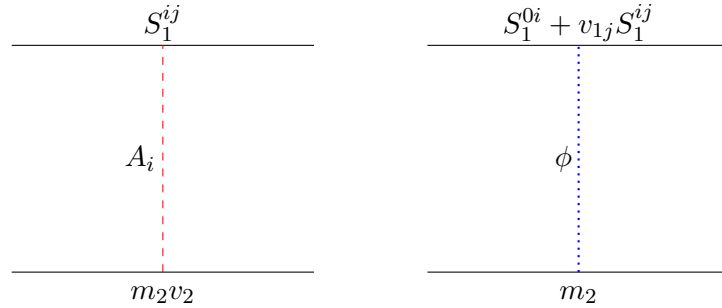


Figure 3: Diagrams representing the LO spin-orbit potential in GR. Diagrams must be supplemented with their  $1 \leftrightarrow 2$  mirror image. Dashed red line represent a  $A_i$ -polarised longitudinal mode, blue dotted lines are  $\phi$ -modes.

The sum of the exchange of gravitational modes with  $A_i$  and  $\phi$  polarisations reported in fig. 3, with vertices given by the Lagrangian (24) gives ( $\vec{r} \equiv \vec{x}_1 - \vec{x}_2$ ) for the LO spin-dependent (*spin-orbit*) potential

$$V_{SO}^{(LO)} = 2 \frac{G_N m_2}{r^3} \vec{S}_1 \cdot (\vec{r} \times \vec{v}) + (\kappa - 1) \frac{G_N m_2}{r^3} \vec{S}_1 \cdot (\vec{r} \times \vec{v}_1) + 1 \leftrightarrow 2. \quad (25)$$

After substituting the covariant SSC (22) with  $\kappa = 1$  one obtains a different result than the classical one [22, 24, 25] which implicitly uses  $\kappa = 1/2$ , however things reconcile at the level of the equation of motions. Indeed using the covariant SSC (i.e.  $\kappa = 1$ ), the spin equations of motion, which are first order, are obtained by using the second of the eqs. (20), then applying the SSC, giving:

$$\dot{S}_1^i = \frac{1}{2} \epsilon^{ijk} \left\{ V_{SO}^{(L)}, S_{1jk} \right\} = \frac{G_N m_2}{r^2} \left[ \vec{S}_1 \times (\hat{n} \times (2\vec{v}_2 - \vec{v}_1)) + \hat{n} \times (\vec{v}_1 \times \vec{S}_1) \right]^i, \quad (26)$$

which implies that the norm of  $\vec{S}_1$  is not conserved, since  $\dot{\vec{S}}_1$  is not perpendicular to  $\vec{S}_1$ . The previous result can be recast into the standard one by performing the  $O(v^2)$  shift of the spin variable according to

$$\vec{S}_a \rightarrow \left( 1 - \frac{v_a^2}{2} \right) \vec{S}_a + \frac{\vec{v}_a}{2} (\vec{v}_a \cdot \vec{S}_a), \quad (27)$$

for  $a = 1, 2$ . The shift (27) (together with the shift (23) to be used for  $\kappa = 1$  only) recast the non-canonical Poisson brackets into canonical ones, finally obtaining a spin vector

with constant norm (neglecting absorption effects [26]), and whose derivative at LO, after substituting the center of mass relationships

$$\vec{v}_1 = \frac{m_2}{M}\vec{v}, \quad \vec{v}_2 = -\frac{m_1}{M}\vec{v}, \quad (28)$$

is given by the standard form [27, 28]

$$\frac{d\vec{S}_1}{dt} = \frac{G_N}{r^3} \left[ 2 + \frac{3m_2}{2m_1} \right] \vec{L} \times \vec{S}_1, \quad (29)$$

being  $\vec{L} \equiv \mu \vec{r} \times \vec{v}$  the Newtonian orbital angular momentum. The result in eq. (29) could have been obtained straightforwardly by substituting relations (28) and  $\kappa = 1/2$  into the potential (25) and then applying canonical Poisson brackets, without the shifts (23) and (27) [22].

Eq. (29) is responsible for the precession of the spin around the orbital angular momentum<sup>4</sup> with angular velocity  $\Omega_S \sim v^3/r$ , i.e. the precession time scale is longer by a factor  $v^{-2}$  than the orbital scale  $r/v$  but shorter than the typical dissipation time-scale  $\eta^{-1}r/v^6$ .

Finally, from the potential (25) and the world-line coordinate shift (23) one can derive the Newtonian equation of motion including effects linear in spin for the relative acceleration of two point-particles at LO in  $v$  [27]:

$$\vec{a} = -\frac{G_N M \vec{r}}{r^3} + 2\frac{G_N}{r^3} \left[ 2 \left( \vec{S}_m \times \vec{v} \right) + 3\frac{\vec{r} \cdot \vec{v}}{r^2} \left( \vec{r} \times \vec{S}_m \right) + 3\frac{\vec{r}}{r^2} \left( \vec{S}_m \cdot \left( \vec{r} \times \vec{v} \right) \right) \right], \quad (30)$$

where  $\vec{S}_m \equiv \left( 1 + \frac{3m_2}{4m_1} \right) \vec{S}_1 + \left( 1 + \frac{3m_1}{4m_2} \right) \vec{S}_2$ . Also in this case the equation of motion (30) can be obtained straightforwardly from the potential (25) with  $\kappa = 1/2$ .

## 2. Spin terms in radiation emission in GR

The lowest order spin-dependent source coupling to  $\sigma_{ij}$  is given by the diagrams in fig. 4. The first diagram does not involve any field propagator, hence it can be directly read from the Lagrangian, and its leading contribution from the  $\sim S^{ij}\sigma_{ik,j}v^j$  term in eq. (24) is of *magnetic* quadrupole type

$$\mathcal{L}_{rad-JS} = \frac{1}{2} S_{1ij} \frac{\sigma_{jk,i}}{m_{Pl}} v_1^k + 1 \leftrightarrow 2 = \frac{1}{4} \left( S_1^i x_1^j + S_1^j x_1^i + 1 \leftrightarrow 2 \right) \frac{\epsilon^{ikl}}{2m_{Pl}} \left( \dot{\sigma}_{ik,l} - \dot{\sigma}_{il,k} \right), \quad (31)$$

<sup>4</sup> The orbital angular momentum is usually larger than individual spins, unless  $\eta \ll 1$  and  $v \lesssim 1$ .

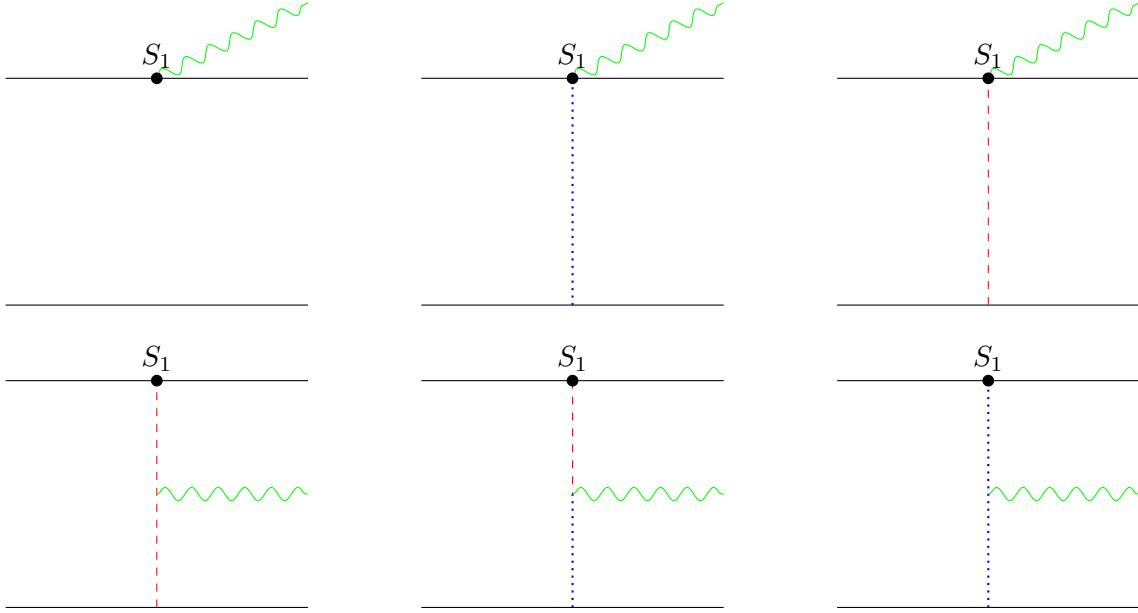


Figure 4: Diagrams determining (part of) the LO spin terms in gravitational radiation emission. The first one contributes at LO to the magnetic quadrupole, the remaining ones to the electric quadrupole. Additional contribution comes from the expression of the radiative multipoles in terms of the energy-momentum tensor, see app. A.

implying by comparison with eq. (14) that the spinning part of the magnetic quadrupole  $J^{ij}$  is

$$J_S^{ij} = \frac{3}{4} \sum_a (S_a^i x_a^j + S_a^j x_a^i)_{TF} , \quad (32)$$

where “ $TF$ ” stands for trace-free part.

The first diagram in fig. 4 also includes the  $\sim S^{0i} \dot{\sigma}_{ij} v^j$  interaction from the Lagrangian (24) which contributes to the electric quadrupole coupling as

$$\begin{aligned} \mathcal{L}_{rad-QSI} &= \left[ \frac{1}{2} \frac{d}{dt} (S_1^{i0} v_1^j + S_1^{j0} v_1^i) + 1 \leftrightarrow 2 \right] \frac{\sigma_{ij}}{2m_{Pl}} \\ &= -\frac{\kappa G_N m_2^2}{2 M r^3} \left[ (\vec{v} \times \vec{S}_1)^i r^j + (\vec{r} \times \vec{S}_1)^i v^j + i \leftrightarrow j \right] \frac{\sigma_{ij}}{2m_{Pl}} + 1 \leftrightarrow 2 , \end{aligned} \quad (33)$$

where in the second line the equation of motion (10) and the center of mass relationships (28) have been used.

The 5 remaining diagrams in fig. 4 contribute to the electric quadrupole, the leading

contribution is of order  $v$  with respect to (31) giving in total:

$$\begin{aligned}
\mathcal{L}_{rad-QSII} &= \frac{G_N m_2}{r^3} \left\{ - \left[ \left( \frac{\kappa + 3}{2} \vec{v}_1 - 2\vec{v}_2 \right) \times S_1 \right]^i r^j - \frac{1}{2} \left( \vec{r} \times \vec{S}_1 \right)^i v_1^j \right. \\
&\quad \left. + 3r^i (\vec{r} \cdot \vec{v}) \left( \vec{r} \times \vec{S}_1 \right)^j + \frac{3}{2} r^i r^j \left[ \left( \vec{r} \times ((1 + \kappa) \vec{v}_1 - 2\vec{v}_2) \right) \cdot \vec{S}_1 \right] \right\} \frac{\sigma_{ij}}{m_{Pl}} + 1 \leftrightarrow 2 \\
&= \frac{G_N m_2}{M r^3} \left\{ - \left( \frac{\kappa + 3}{2} m_2 + 2m_1 \right) (\vec{v} \times S_1)^i r^j - \frac{1}{2} \left( \vec{r} \times \vec{S}_1 \right)^i v^j \right. \\
&\quad \left. + 3M r^i (\vec{r} \cdot \vec{v}) \left( \vec{r} \times \vec{S}_1 \right)^j + \frac{3}{2} r^i r^j ((1 + \kappa) m_2 + 2m_1) (\vec{r} \times \vec{v}) \cdot \vec{S}_1 \right\} \frac{\sigma_{ij}}{m_{Pl}} + 1 \leftrightarrow 2,
\end{aligned} \tag{34}$$

where in the last passage the center of mass relationships (28) have been inserted.

Eqs. (33) and (34) give the explicit form of the linear coupling of the sources to  $\sigma_{ij}$ , i.e. of  $T^{ij}$ , as per eq. (8). To check that this result coincides with the standard one eq. (11), one has to use the conservation of the energy momentum tensor (equivalent to the source equations of motion) eq. (13) to reproduce the quadrupole moment from  $T_{ij}$  via the standard GR textbook trick reported in app. A.

Indeed the linear-in-spin mass quadrupole

$$Q_S^{ij} \equiv \int_V T^{00}|_S x^i x^j = (S_1^{i0} x_1^j + S_1^{j0} x_1^i) + 1 \leftrightarrow 2, \tag{35}$$

satisfies  $\ddot{Q}^{ij} = 2 \int_V T^{ij}$  on the equations of motion with  $T^{ij}$  obtained from  $\mathcal{L}_{rad-QSI+II} = \frac{1}{2} T^{ij} \sigma_{ij} / m_{Pl}$ , i.e. from the sum of eqs. (33) and (34), considering the contribution of the equation of motion (30) that needs to be used to cast (9) into (11), using  $\kappa = 1/2$ .<sup>5</sup>

For the spin-dependent part however, the radiative quadrupole  $I^{ij}$  coupling to the Riemann as per eq. (11) does not coincide with the mass quadrupole even at LO, as it is rather given by [25]

$$\begin{aligned}
I^{ij}|_S &= \int_V \left( T^{00} + T^{ll} - \frac{4}{3} \dot{T}^{0l} x^l \right) (x^i x^j)_{TF} \Big|_S \\
&= \left\{ (\kappa + 1) \left[ \left( \vec{v}_1 \times \vec{S}_1 \right)^i r^j \right] - \frac{2}{3} \left[ \left( \vec{v}_1 \times \vec{S}_1 \right)^i \vec{r}_1^j + \left( \vec{r}_1 \times \vec{S}_1 \right)^i \vec{v}_1^j \right] + i \leftrightarrow j \right\}_{TF} + 1 \leftrightarrow 2,
\end{aligned} \tag{36}$$

where for  $T^{0l}$ ,  $T^{ij}$  we inserted their LO expressions that can be read directly from the Lagrangian (6):  $\frac{1}{4} S_a^{ij} F_{ji}$  and  $\frac{1}{2} S_a^{ik} v_a^j \sigma_{ij,k}$ .

Had not we used the GR equations of motions, we would have obtained the coupling

$$\mathcal{L}_{rad} = \frac{\sigma_{ij}}{2m_{Pl}} \int_V \left[ T^{ij} + \frac{1}{7} \frac{d^2}{dt^2} \left( \frac{2}{3} T^{ll} x^i x^j + \frac{11}{6} T^{ij} r^2 - T^{il} x^l x^j - T^{jl} x^l x^i \right) \right]_{TF}, \tag{37}$$

<sup>5</sup> We use here the baryonic SSC for simplicity, to avoid the complication of a non-standard Poisson algebra, see eq. (A2) for details.

which is equivalent to (11) in GR, see app. A for details and derivation.

In total one has the electric quadrupole coupling, for  $\kappa = 1/2$  and in the center of mass:<sup>6</sup>

$$\mathcal{L}_{rad-QS} = -\frac{1}{6} \frac{G_N m_2^2}{M r^3} \left[ \left( \vec{r} \times \vec{S}_1 \right)^i v^j + \left( \vec{v} \times \vec{S}_1 \right)^i r^j - \frac{3}{2} \frac{(\vec{r} \cdot \vec{v})}{r^2} \left( \vec{S}_1 \times \vec{r} \right)^i r^j \right] \frac{\sigma_{ij}}{m_{Pl}} + 1 \leftrightarrow \mathfrak{A}38$$

### III. RESULTS FOR RIEMANN<sup>4</sup> TERMS

To systematically show the results when short-scale deviations from GR are present, we present separately the effects of the terms  $\mathcal{C}^2$ ,  $\mathcal{C}\tilde{\mathcal{C}}$  and  $\tilde{\mathcal{C}}^2$  of eq. (1).

#### A. $\mathcal{C}^2$

The Riemann to the fourth power addition to the GR Lagrangian introduce 4-point interactions that change both the potential and the emission formulae. The spin-less LO corrections depending on the  $\mathcal{C}^2$  terms can be derived from the contributions of diagrams in fig. 5 for the potential, and fig. 7 for the emission, which gives  $G_N^2$  (or equivalently  $v^4$ ) corrections with respect to the LO energy and emitted radiation flux.

Considering effects linear in spin with the lowest number of velocity factors (i.e. the lowest PN order), one has to compute the four-point vertex involving the lowest number of time derivative and velocities (and neglecting terms vanishing on the equations of motion), hence one can approximate

$$\begin{aligned} \mathcal{C} \simeq \frac{8}{m_{Pl}^2} & \left\{ (\partial_i \partial_j \phi) (\partial^i \partial^j \phi) + \left( \partial_i \dot{A}_j (\partial^i \partial^j \phi) - (\partial_i \partial_j A^j) \partial_i \dot{\phi} \right) - \frac{1}{2} (\ddot{\sigma}_{ij} + \nabla^2 \sigma_{ij}) (\partial^i \partial^j \phi) \right. \\ & + (\partial_i \partial_j \phi) \partial^i \partial_k \left( \sigma^{jk} - \frac{\delta^{jk}}{2} \sigma \right) + \frac{1}{2} \partial_i (\partial_k A_j - \partial_j A_k) \partial_k \dot{\sigma}_{ij} \\ & \left. + \frac{1}{4} (\partial_i \partial_j A_k) \partial_i (\partial_j A_k - \partial_k A_j) + \frac{1}{8} (\partial_i \partial_j \sigma_{kl}) [(\partial_i \partial_j \sigma_{kl}) + (\partial_k \partial_l \sigma_{ij}) - 2 (\partial_i \partial_k \sigma_{jl})] + \dots \right\}, \end{aligned} \quad (39)$$

$$\begin{aligned} \mathcal{C}^2 \simeq \frac{64}{m_{Pl}^4} & (\partial_m \partial_n \phi) (\partial^m \partial^n \phi) \times \left\{ (\partial_i \partial_j \phi) (\partial_i \partial_j \phi) + 2 \left[ \partial_i \dot{A}_j (\partial^i \partial^j \phi) - (\partial_i \partial_j A^j) \partial_i \dot{\phi} \right] \right. \\ & - (\ddot{\sigma}_{ij} + \nabla^2 \sigma_{ij}) (\partial^i \partial^j \phi) + 2 (\partial_i \partial_j \phi) \partial^i \partial_k \left( \sigma^{jk} - \frac{\delta^{jk}}{2} \sigma \right) + \partial_i (\partial_k A_j - \partial_j A_k) \partial_k \dot{\sigma}_{ij} \\ & \left. + \frac{1}{4} (\partial_i \partial_j \sigma_{kl}) [(\partial_i \partial_j \sigma_{kl}) + (\partial_k \partial_l \sigma_{ij}) - 2 (\partial_i \partial_k \sigma_{jl})] + \dots \right\}. \end{aligned} \quad (40)$$

---

<sup>6</sup> Note that using the LO expression for the linear in spin  $T^{ij}$  the term  $\frac{d^2}{dt^2} (T^{il} x^l x^j + T^{jl} x^l x^i)$  in eq. (37) vanishes.

Note that in the spin-less case the potential gravitational mode  $\phi, A_i, \sigma_{ij}$  couples to world-line with respectively 0,1,2 powers of velocity, in the spinning case  $A_i$  couples without time derivative or power of velocity, whereas  $\phi$  and  $\sigma_{ij}$  require one power of velocity or a time derivative, see eq. (24).

### 1. Potential

#### No spin

The lowest order spin-dependent contributions to the potential due to the  $\mathcal{C}^2$  term are given by the processes represented in fig. 5, plus their mirror image under  $1 \leftrightarrow 2$  exchange. They correspond to the the “cross” and “peace/log” diagrams as they were named in [6].

The LO contribution to the potential is, see app. B1 a for details, first computed in eq. (5.9) of [6]

$$V_\Lambda = -V_N \frac{512}{(\Lambda r)^6} \left( \frac{G_N m_2}{r} \right)^2 + 1 \leftrightarrow 2, \quad (41)$$

where  $V_N$  is the standard Newtonian potential, modifying the spin-independent part of the equation of motion to

$$\vec{a}_\Lambda = \vec{a}_{1\Lambda} - \vec{a}_{2\Lambda} = -\frac{G_N M \vec{r}}{r^3} \left[ 1 - \frac{4608}{(\Lambda r)^6} \frac{G_N^2 (m_1^2 + m_2^2)}{r^2} \right]. \quad (42)$$

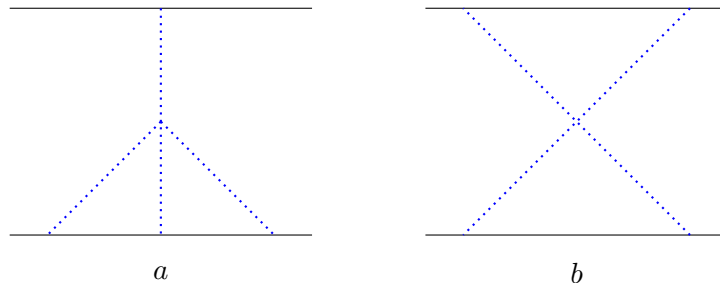


Figure 5: Diagrams representing the leading corrections to the non-spinning potential from  $\mathcal{C}^2$  interactions (blue dotted lines represent  $\phi$  propagators). The cross diagram vanishes. The  $a$  diagram must be complemented by its mirror image under particle exchange.

#### Spin

The LO, linear-in-spin contribution to the potential can be derived by computing the diagrams in fig. 6, see app. B2 a for details. They are all diagrams with 1 power of the spin and

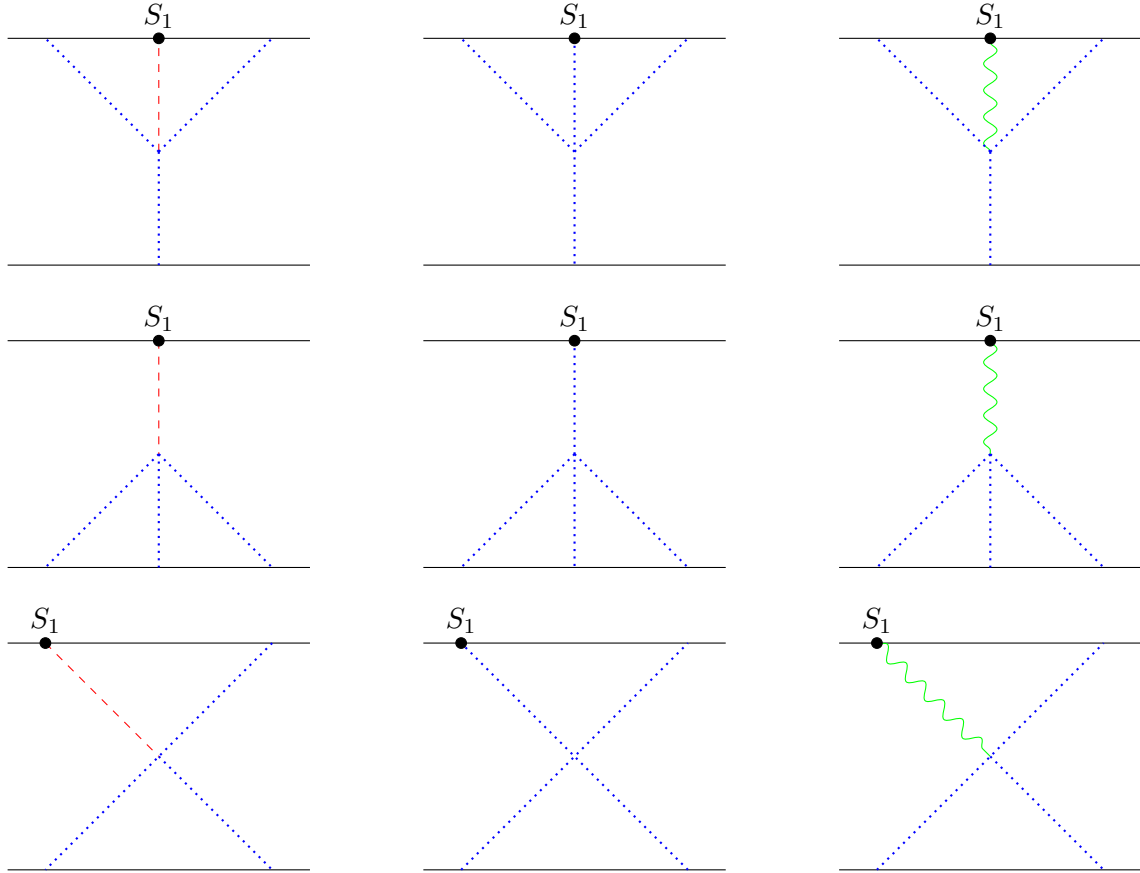


Figure 6: Diagrams representing the leading corrections to the linear-in-spin potential from  $\mathcal{C}^2$  interactions. Blue dotted lines represent  $\phi$  propagators, red dashed for  $A$ , green wavy for  $\sigma$ . All cross diagrams vanish, as well as the first (diagram with the field  $A$  coupling to  $S_1$ ) and third ( $\sigma$  coupling to  $S_1$ ) diagram on the second line. Diagrams obtained by exchanging particles 1 and 2 should be added.

1 power of the velocity of any of the two particles (there are no spin-dependent contributions for  $\vec{v}_1 = \vec{v}_2 = 0$ ).

Overall they give the following potential

$$V_{\Lambda S_1} = -(1 + \kappa) \frac{4608}{(\Lambda r)^6} \vec{S}_1 \cdot (\vec{r} \times v_1) \frac{G_N^3 m_2 (m_1^2 + m_2^2)}{r^5}, \quad (43)$$

leading to a modification of the equation of motion

$$\vec{a}_{\Lambda S} = -6912 \frac{G_N^3 (1 - 2\eta) M^2}{\Lambda^6 r^{11}} \left[ 2\vec{S}_C \times \vec{v} + 11 \frac{\vec{r} \cdot \vec{v}}{r^2} (\vec{r} \times \vec{S}_C) + 11 \frac{\vec{r}}{r^2} (\vec{S}_C \cdot (\vec{r} \times \vec{v})) \right], \quad (44)$$

which is independent of  $\kappa$  and where the definition  $\vec{S}_C \equiv \frac{1}{M} \left( \frac{m_2^2}{m_1} \vec{S}_1 + \frac{m_1^2}{m_2} \vec{S}_2 \right)$  has been used.



The spin equation of motion with the contribution of the  $\mathcal{C}^2$  interaction are obtained following the same procedure as the one used in sec. II to derive the LO spin-orbit coupling, to obtain the  $\mathcal{C}^2$  correction

$$\left. \frac{d\vec{S}_1}{dt} \right|_{\Lambda} = -\frac{6912}{(\Lambda r)^6} \frac{G_N^3 (m_1^2 + m_2^2)}{r^5} \left( \frac{m_2}{m_1} \right) \vec{L} \times \vec{S}_1, \quad (45)$$

which is independent of the SSC chosen (i.e.  $\kappa = 0$  or  $\kappa = 1/2$ ).

## 2. Radiation

### No spin

The relevant diagram for the  $\mathcal{C}^2$  contribution to the emission from non-spinning sources is given in fig. 7, first computed in eq. (6.6) of [6], and it is worth

$$L_{fig.7} = 1344 \frac{G_N^2 m_1^2 m_2}{\Lambda^6 r^8} r^i r^j \frac{\ddot{\sigma}_{ij}}{2m_{Pl}} + 1 \leftrightarrow 2 = 1344 \frac{G_N^2 \eta M^3}{(\Lambda r)^6} n^i n^j \frac{\ddot{\sigma}_{ij}}{2m_{Pl}}, \quad (46)$$

with  $n^i \equiv \frac{r^i}{r}$ , where to simplify the calculations we work in the Transverse Traceless (TT) gauge, which is valid only for the radiative field (i.e. on-shell and in vacuum), enabling to write  $\ddot{\sigma}_{ij} = \nabla^2 \sigma_{ij} = -2R_{0i0j} m_{Pl}$  and  $\dot{\sigma}_{ij,k} - \dot{\sigma}_{ik,j} = 2R_{0ijk} m_{Pl}$ , see app. C 1 a for details.

To express the leading radiative coupling in terms of the quadrupole, one needs to combine eq. (46) with the contribution from the modified equation of motion (42), that enters the game when expressing the radiative coupling (9) in terms of quadrupole derivatives, see eq. (A2) for details. In total one has

$$L_{rad-\Lambda} = \left[ \frac{d^2}{dt^2} \left( \frac{Q^{ij}}{2} + 1344 \frac{G_N^2 \eta M^3}{(\Lambda r)^6} n^i n^j \right) - 4608 \frac{G_N^3 M^4 \eta (1 - 2\eta)}{\Lambda^6 r^9} n^i n^j \right] \frac{\sigma_{ij}}{2m_{Pl}}. \quad (47)$$

Beside the shift in the quadrupole coupling given by (46), we see that the non-GR structure of our effective theory, via non-conservation of the energy-momentum tensor, introduces terms in radiative interaction which do not have a multipolar structure, as the last term in square bracket in eq. (47). In terms of PN scaling, the  $\Lambda$  dependent terms in (47) are of the same order (remember that  $\frac{d}{dt} \sim \frac{v}{r}$ ):  $2\text{PN} \times (\Lambda r)^{-6}$  with respect to the leading term (9).

### Spin

The contribution to radiation emission processes introduced by the quartic interaction due to the  $\mathcal{C}^2$  term can be distinguish in magnetic and electric ones. Contrarily from the non-spinning case, the spinning LO emission process is of *magnetic* type, and described by the

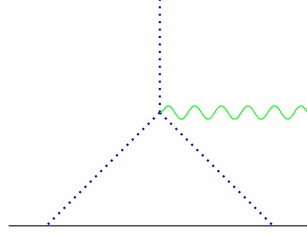


Figure 7: Leading  $\mathcal{C}^2$  correction to the emission process for non-spinning sources. Blue dotted lines are longitudinal modes exchanged between the sources, green wavy line the radiative gravitational mode.

processes reported in fig. 8, the ones of electric type are reported in fig. 9 and are  $O(v)$  with respect to the former.

Indeed, as it can be seen from the scaling of the world-line (24) and bulk (40) couplings, the processes in fig. 8 give a contribution to the *magnetic* quadrupole which is  $2\text{PN} \times (\Lambda r)^{-6}$  order with respect to the leading GR magnetic quadrupole, whereas the electric emission processes in fig. 9 contribute at order  $2.5\text{PN} \times (\Lambda r)^{-6}$  with respect to the leading electric quadrupole in GR, see fig. 2: as a result the contribution from  $\mathcal{C}^2$  terms to the radiation flux  $F$  in eq. (15) from the magnetic and the electric quadrupole is of the same order, since for the spin-less part  $J_{ij} \sim v \times Q_{ij}$ .

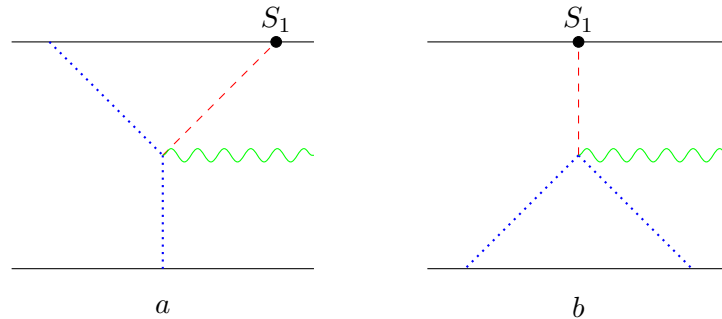


Figure 8: Diagrams representing the leading *magnetic* contribution to radiation emission process from  $\mathcal{C}^2$  interaction, generated by bulk terms  $\sim (\partial_m \partial_n \phi)^2 \times \partial_i \partial_j A_k R^{0ijk}$ . Blue dotted lines represent  $\phi$  propagators, red dashed for  $A_i$ , green wavy for  $\sigma_{ij}$ .

The diagrams in fig. 8 represents the linear-in-spin  $\mathcal{C}^2$  contributions to the magnetic

quadrupole, giving, see app. C 2 a for details,

$$\mathcal{L}_{fig.8} = \frac{384}{(\Lambda r)^6} \frac{G_N^2 m_2}{r^2} \left[ (4m_1 + 5m_2) (S_1^i r^j + S_1^j r^i) - 2(5m_1 + 8m_2) n^i n^j (\vec{r} \cdot \vec{S}_1) \right] \mathcal{B}_{ij}, \quad (48)$$

which corrects the magnetic quadrupole according to

$$J^{ij}|_{LO,\Lambda S_1} = \frac{3}{4} (S_1^i r^j + S_1^j r^i)_{TF} \times \left[ 1 + 512 \frac{G_N^2 m_2}{\Lambda^6 r^8} (4m_1 + 5m_2) \right] - 768 (n^i n^j)_{TF} (\vec{r} \cdot \vec{S}_1) \frac{G_N^2 m_2}{\Lambda^6 r^8} (5m_1 + 8m_2) + 1 \leftrightarrow 2, \quad (49)$$

which is again a  $2\text{PN} \times (\Lambda r)^{-6}$  correction to the LO.

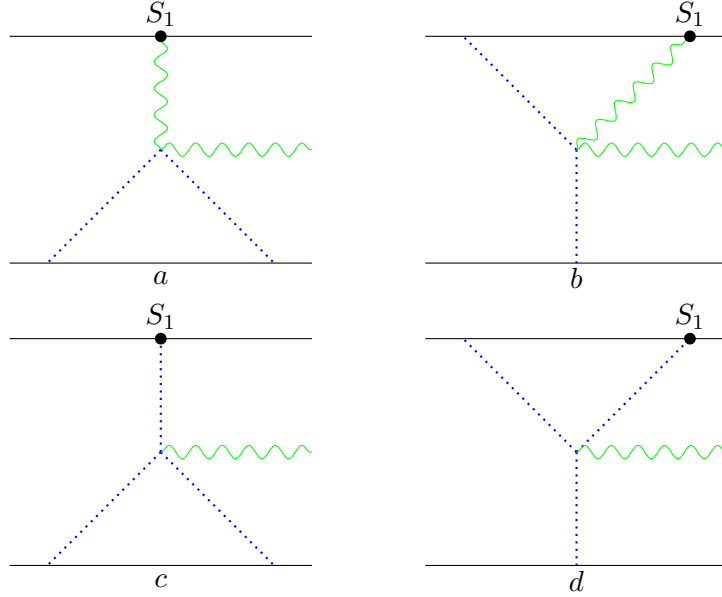


Figure 9: Diagrams representing the leading *electric* contribution to radiation emission process from  $\mathcal{C}^2$  interaction, generated by bulk terms  $\sim (\partial_m \partial_n \phi)^2 \partial_i \partial_j \phi (R_{0i0j} + \delta^{kl} R_{ikjl})$ . Blue dotted lines represent  $\phi$  propagators, green wavy for  $\sigma$ .

From fig. 9 one gets the linear-in-spin  $\mathcal{C}^2$  corrections to the electric quadrupole, see app. C 2 a for detailed computations,

$$\begin{aligned} \mathcal{L}_{fig.9} = \frac{192}{(\Lambda r)^6} \frac{G_N^2 m_2}{r^2} \left\{ (5m_1 + 8m_2) n^i (\hat{n} \cdot \vec{v}_1) (\vec{S}_1 \times \vec{r})^j - (m_1 + 4m_2) v_1^i (\vec{S}_1 \times \vec{r})^j \right. \\ \left. - (15 + 14\kappa) (m_1 + m_2) r^i (\vec{S}_1 \times \vec{v}_1)^j - 56 (1 + \kappa) (m_1 + m_2) n^i n^j \left[ \vec{S}_1 \cdot (\vec{r} \times \vec{v}_1) \right] \right\} R_{0i0j}. \end{aligned} \quad (50)$$

For the linear-in-spin part, like in the non-spinning case eq. (47), the radiative coupling receives contributions from the modification of the equation of motion eq. (44) as per eq. (A2)

$$L_{rad-\Lambda S} = -\frac{I^{ij}}{2}\mathcal{E}_{ij} + 6912\frac{G_N^3 M^3 \eta(1-2\eta)}{\Lambda^6 r^{11}} r^i \left\{ 2\left(\vec{S}_C \times \vec{v}\right)^j + 11\frac{\vec{r} \cdot \vec{v}}{r^2} \left(\vec{r} \times \vec{S}_C\right)^j + 11\frac{r^j}{r^2} \left[\vec{S}_C \cdot (\vec{r} \times \vec{v})\right] + i \leftrightarrow j \right\} \frac{\sigma_{ij}}{2m_{Pl}}, \quad (51)$$

and the electric quadrupole  $I_{ij}$  is modified to:

$$I_{ij}|_{S_1} = \frac{m_2^2}{M^2} \left\{ \left(\vec{v} \times \vec{S}_1\right)^i r^j \left[ 2\kappa + \frac{2}{3} + \frac{192}{(\Lambda r)^6} \frac{G_N^2 M^2}{r^2} (15 + 14\kappa) \right] + \left(\vec{r} \times \vec{S}_1\right)^i v^j \left( -\frac{4}{3} + \frac{192}{(\Lambda r)^6} \frac{G_N^2 M (m_1 + 4m_2)}{r^2} \right) + \frac{192}{(\Lambda r)^6} \frac{G_N^2 M}{r^2} \left[ -56M(1 + \kappa) n^i n^j \left(\vec{S}_1 \cdot (\vec{r} \times \vec{v})\right) + (5m_1 + 8m_2) n^i (\hat{n} \cdot \vec{v}) \left(\vec{S}_1 \times \vec{r}\right)^j \right] + 1 \leftrightarrow 2 \right\}_{STF}. \quad (52)$$

where “*STF*” stand for symmetric (in  $i, j$ ) and trace-free part.

## B. $\mathcal{C}\tilde{\mathcal{C}}$

The  $\tilde{\mathcal{C}}$  term violates both parity and time-reversal invariance, the explicit expression of  $\tilde{\mathcal{C}}$  and  $\mathcal{C}\tilde{\mathcal{C}}$ , limited to the terms with lower number of time derivatives of interest for this work, are

$$\tilde{\mathcal{C}} \simeq 4\frac{\epsilon_{jkl}}{m_{Pl}^2} \left[ -4(\partial_i \partial_j \phi)(\partial_i \partial_k A_l) + \ddot{\sigma}_{ij}(\partial_i \partial_k A_l) + \partial_k \partial_n \sigma_{ml} \partial_j (\partial_n A_m - \partial_n A_n) - 4(\partial_i \partial_j \phi) \partial_l \dot{\sigma}_{ik} + \partial_n \dot{\sigma}_{jm} \partial_k (\partial_m \sigma_{ln} - \partial_n \sigma_{lm}) \right], \quad (53)$$

$$\begin{aligned} \mathcal{C}\tilde{\mathcal{C}} \simeq & 32\frac{\epsilon_{jkl}}{m_{Pl}^4} \left[ (\partial_m \partial_n \phi)(\partial_m \partial_n \phi) + \frac{1}{2}\epsilon_{amn}\epsilon_{ars}(\partial_c \partial_m A_n) \partial_r \dot{\sigma}_{cs} + \frac{1}{4}(\partial_m \partial_n A_c) \partial_m (\partial_n A_c - \partial_c A_n) \right. \\ & \left. + (\partial_m \dot{A}_n) (\partial_m \partial_n \phi) - (\partial_m \partial_n A_n) (\partial_m \dot{\phi}) + (\partial_c \partial_m \phi) \partial_c \partial_n \left( \sigma_{mn} - \frac{1}{2}\delta_{mn}\sigma \right) \right] \\ & \times \left[ -4(\partial_i \partial_j \phi)(\partial_i \partial_k A_l) + \ddot{\sigma}_{ij}(\partial_i \partial_k A_l) + \partial_k \partial_n \sigma_{ml} \partial_j (\partial_n A_m - \partial_m A_n) \right. \\ & \left. - 4(\partial_i \partial_j \phi) \partial_l \dot{\sigma}_{ik} + (\partial_l \dot{\sigma}_{ik}) \epsilon_{imn}\epsilon_{jrs} \partial_n \partial_s \sigma_{mr} + \dots \right], \quad (54) \end{aligned}$$

### 1. Potential

#### No spin

The  $\mathcal{C}\tilde{\mathcal{C}}$  contribution to the conservative potential vanishes at all orders in the spin-less

case, as this interaction involves a Levi-Civita tensor which has to be contracted with three linearly independent vectors to generate a scalar potential. However for a non-spinning binary system all vectors available lie in the orbital plane, hence the  $\mathcal{CC}$  contribution to the potential vanishes.

### Spin

In the spinning case diagrams in fig. 10 give, see app. B 2 b for details,

$$V_{\Lambda_- S_1} = -4608 \frac{G_N^3 m_1^2 m_2}{r^5 (\Lambda_- r)^6} \vec{r} \cdot \vec{S}_1, \quad (55)$$

which is a  $1.5\text{PN} \times (\Lambda_- r)^{-6}$  correction with respect to the leading spin term in the potential eq. (25), the half-integer relative order due to parity violation nature of the term, modifying the spin equation of motion per

$$\left. \frac{d\vec{S}_1}{dt} \right|_{\Lambda_-} = -4608 \frac{G_N^3 m_1^2 m_2}{r^5 (\Lambda_- r)^6} \vec{r} \times \vec{S}_1, \quad (56)$$

which induces a perturbation into spin equation of motion with characteristic frequency given by the orbital frequency. This is a distinctive effect generated by the parity violating Lagrangian which is qualitative different from other modifications.

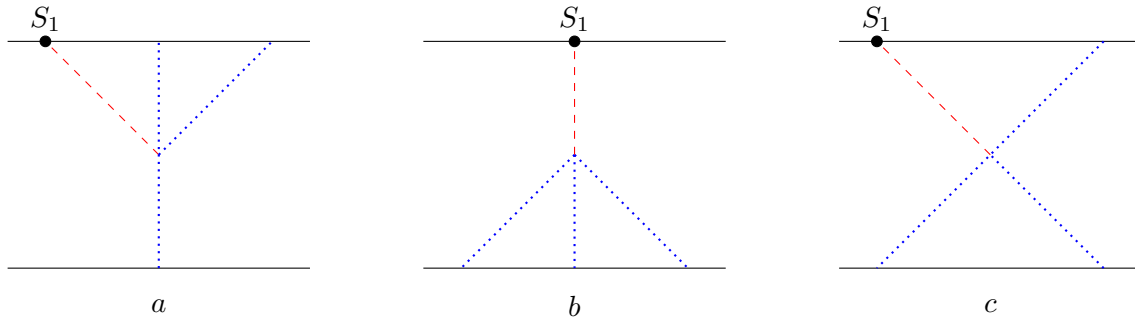


Figure 10: Diagrams representing the leading corrections to the spinning potential from  $\mathcal{CC}$  interactions (blue dotted lines represent  $\phi$  propagators, red dashed  $A_i$  ones) at 2PN order with respect to leading GR behaviour. Only the first diagram is non-vanishing.

## 2. Emission

### No spin

The parity violating term under consideration couples at lowest order to the magnetic part

of the Riemann via an electric quadrupole in fig. 11a giving a coupling to radiative field, see app. C 1 b for details:

$$L_{fig. 11a} = -\frac{1344}{(\Lambda_- r)^6} \frac{G_N^2 m_1 m_2^2}{r^2} r^i r^j \frac{1}{4} \epsilon_{ikl} (\dot{\sigma}_{jk,l} - \dot{\sigma}_{jl,k}) + 1 \leftrightarrow 2. \quad (57)$$

Note that since at leading order  $\mathcal{B}_{ij}$  couples to  $J^{ij} = \frac{1}{2} \mu v^k x^l \epsilon_{mkl} (\delta^{mi} x^j + \delta^{mj} x^i)$ , eq. (57) represents a 1.5PN electric correction to the magnetic quadrupole. In this case there is no contribution from modified equations of motion, see eq. (A2), as the interaction  $\mathcal{C}\tilde{\mathcal{C}}$  does not affect the conservative dynamics in the non-spinning sector, giving

$$L_{rad-\Lambda-J} = -\left[ \frac{1}{3} (r^i L^j + r^j L^i) + 1344 \frac{\eta G_N^2 M^3}{r^2 (\Lambda_- r)^6} r^i r^j \right] \mathcal{B}_{ij}, \quad (58)$$

which agrees with eq. (6.21) of [6].

The correction to the emission process coupling to the electric part of the Riemann is of 2.5 PN order with respect to the leading radiative electric coupling, and as at leading order  $J_{ij} \sim v \times I_{ij}$  the electric and magnetic terms involving the  $\mathcal{C}\tilde{\mathcal{C}}$  interaction contribute to the flux (15) at the same order.

The contributions to the electric emission processes in fig. 11b,c give

$$L_{fig. 11bc} = 1536 \frac{G_N^2 m_1 m_2^2}{\Lambda_-^6 r^8} r^i \left[ \vec{r} \times \left( \vec{v}_1 + \frac{3}{4} \vec{v}_2 \right) \right]^j \frac{\ddot{\sigma}_{ij}}{2m_{Pl}} + 1 \leftrightarrow 2, \quad (59)$$

which together with the leading order gives an electric radiative coupling

$$L_{rad-\Lambda-I} = -\mu \left( \frac{1}{2} r^i r^j + 768 \frac{G_N^2 M^2 (2 - 7\eta)}{r^2 (\Lambda_- r)^6} r^i L^j \right)_{STF} \mathcal{E}_{ij}. \quad (60)$$

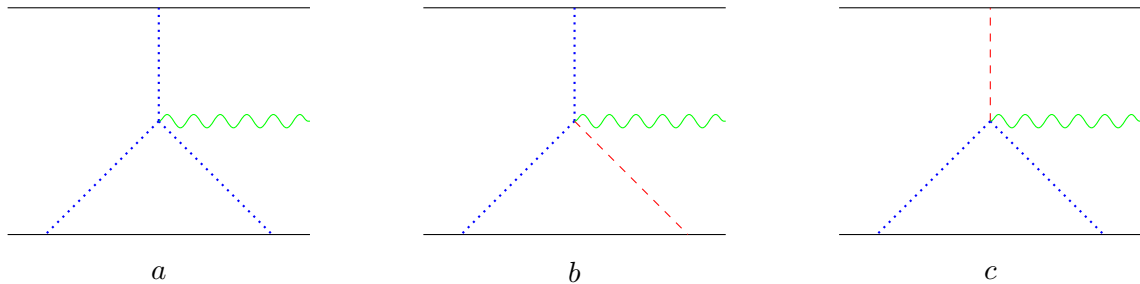


Figure 11: Diagram giving the LO effect of  $\mathcal{C}\tilde{\mathcal{C}}$  on the radiation emission for the non-spinning case. At leading order diagram *a* contributes to the magnetic coupling, *b* and *c* to the electric part.

## Spin

The diagrams giving the leading  $\mathcal{CC}$  electric contribution to radiation in the spinning case are reported in fig. 12, see app. C 2 b for details. The electric type radiation process gives the following Lagrangian coupling

$$L_{fig. 12\mathcal{E}} = 384 \frac{G_N^2 m_2}{r^2 (\Lambda_- r)^6} \left[ (7m_1 + 15m_2) r^i S_1^j - 4(7m_1 + 6m_2) n^i n^j (\vec{r} \cdot \vec{S}_1) \right] \mathcal{E}_{ij}, \quad (61)$$

representing a  $1.5\text{PN} \times (\Lambda_- r)^{-6}$  magnetic type correction to the spin-dependent electric quadrupole which can be read from eq. (38).

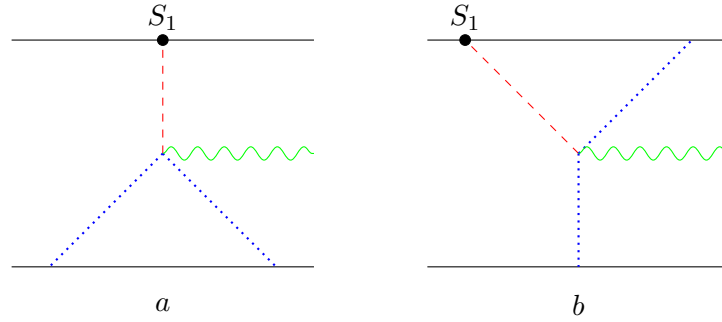


Figure 12: Diagram giving the LO effect of  $\mathcal{CC}$  on the radiation emission for the electric spinning case. They contribute also to the magnetic coupling.

The linear-in-spin magnetic type processes give  $2.5\text{PN} \times (\Lambda_- r)^{-6}$  corrections with respect to the leading order magnetic emission terms, which then induce sub-leading effects in the emission amplitude with respect to (61). However the linear-in-spin term of the electric quadrupole is subleading by a factor of  $v$  with respect to the analog magnetic quadrupole term, hence electric and magnetic  $\mathcal{CC}$  linear-in-spin terms give same order contributions to the flux. In addition to the diagrams in fig. 12, in the magnetic case one has also the diagrams of fig. 13. Overall the magnetic radiative coupling induced by the  $\mathcal{CC}$  term is, see app. C 2 b for details,

$$L_{fig. (12+13)\mathcal{B}} = 24 \frac{G_N^2 m_2}{r^2 (\Lambda_- r)^6} \left\{ \left( \vec{r} \times \vec{S}_1 \right)^i \left[ 2v_1^j (41m_2 + 32m_1) - 16v_2^j (7m_2 + 6m_1) \right] + \right. \\ \left. \left( \vec{r} \times \vec{S}_1 \right)^i \frac{r^j r^m}{r^2} \left[ -2v_{1m} (130m_2 + 61m_1) + 64v_{2m} (8m_1 + 9m_2) \right] \right. \\ \left. - n^i n^j S_1^m \left[ (\vec{r} \times \vec{v}_1)_m (346m_2 + 605m_1) + (\vec{r} \times \vec{v}_2)_m 32 (20m_2 + 23m_1) \right] \right. \\ \left. + r^i \left[ 2 \left( \vec{S}_1 \times \vec{v}_1 \right)^j (27m_2 + 77m_1) + 224 \left( \vec{S}_1 \times \vec{v}_2 \right)^j (m_2 + 2m_1) \right] \right\} \mathcal{B}_{ij}, \quad (62)$$

where  $\kappa = 1/2$  has been used.

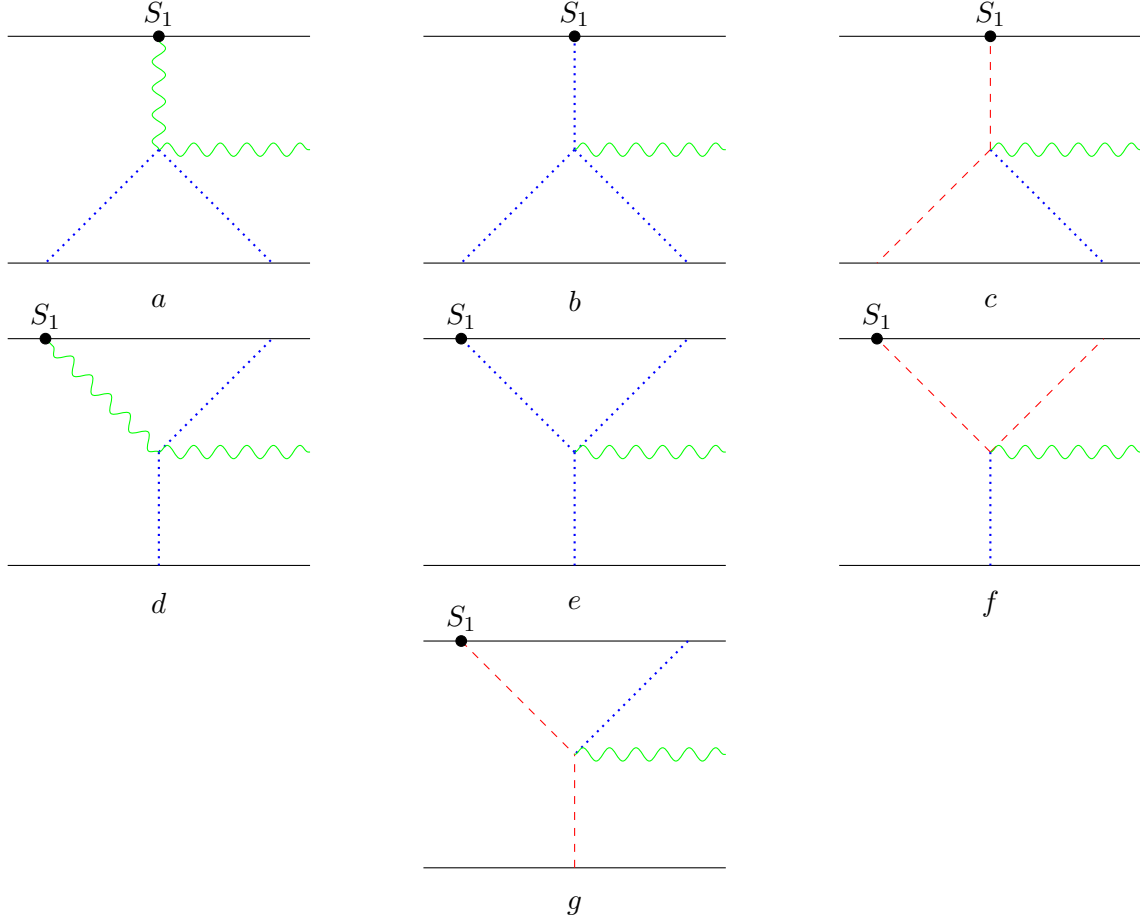


Figure 13: Additional diagrams contributing via  $\mathcal{C}\tilde{\mathcal{C}}$  interaction to the LO radiation emission for the magnetic spinning case.

### C. $\tilde{\mathcal{C}}^2$

While the  $\tilde{\mathcal{C}}$  term violates parity, the  $\tilde{\mathcal{C}}^2$  does not and its expression is given by the square of (53).

#### 1. Potential

##### No spin

The potential interaction mediated by  $\tilde{\mathcal{C}}^2$  vanish in the static limit and it is  $v^2$  with respect to the one mediated by the  $\mathcal{C}^2$ , i.e. a 3PN correction to the Newtonian potential and it will not be computed here.



## Spin

The LO potential mediated by the  $\tilde{\mathcal{C}}^2$  interaction in the spinning case is given by the processes in fig. 14 with the total result, see app. B 2 c for details,

$$L_{pot-\tilde{\Lambda}S_1} = \frac{55296 G_N^3 m_1^2 m_2}{11 r^5 (\tilde{\Lambda} r)^6} [\vec{r} \times (\vec{v}_1 - \vec{v}_2)] \cdot \vec{S}_1, \quad (63)$$

which agrees with eq. (5.18) of [6].

This contribution is analogous to the one of the  $\mathcal{C}^2$  term and it introduces a correction to the spin equation of motion

$$\left. \frac{d\vec{S}_1}{dt} \right|_{\tilde{\Lambda}} = \frac{55296 G_N^3 M m_2}{11 r^5 (\tilde{\Lambda} r)^6} \vec{L} \times \vec{S}_1, \quad (64)$$

analogous to the  $\mathcal{C}^2$  case eq. (45).

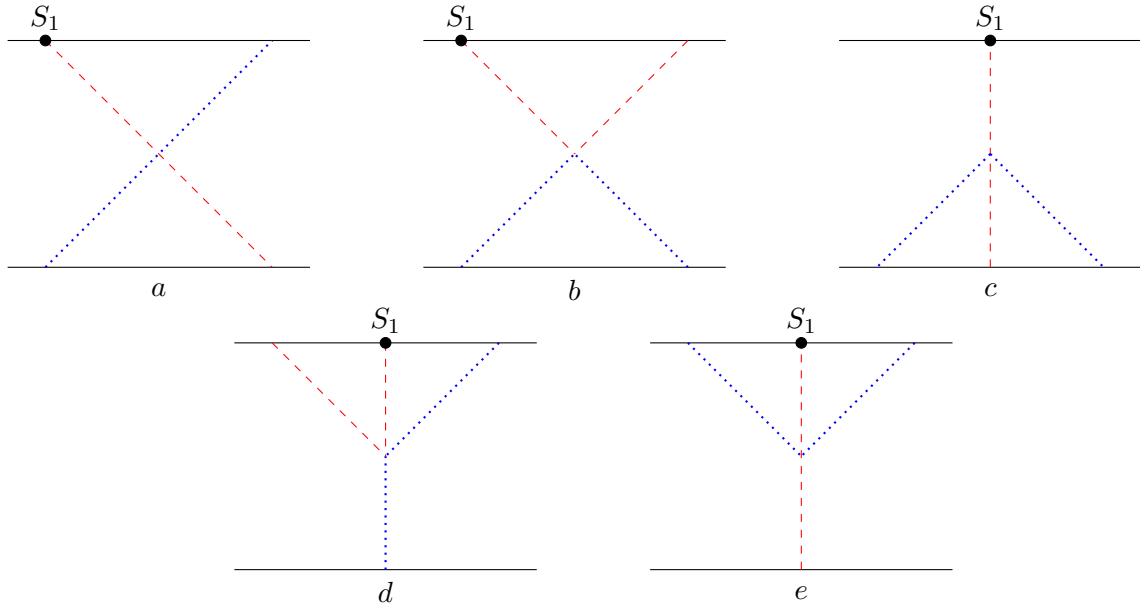


Figure 14: Diagrams representing the correction to the spinning potential mediated by the  $\tilde{\mathcal{C}}^2$  bulk interaction. Diagrams must be supplemented with their mirror images under  $1 \leftrightarrow 2$ . The three diagrams in the first line vanish.

## 2. Emission

### No spin

The radiative interaction due to the  $\tilde{\mathcal{C}}^2$  term are  $v^2$  with respect to the one mediated by the

$\mathcal{C}^2$ , i.e. a 3PN correction to the quadrupole formula and it will not be computed here.

### Spin

The radiative, linear-in-spin processes contribute to both the electric and magnetic coupling, each being 2PN order  $\times (\tilde{\Lambda}r)^{-6}$  the respective leading order one (38) and (31). From fig. 15, see app. C 2 c for details, one gets the Lagrangian contributions to the electric-type radiative couplings

$$L_{fig.15} = \frac{384}{(\tilde{\Lambda}r)^6} \frac{G_N^2 \mu}{r^2} \left\{ -2(94m_1 + 43m_2) n^i n^j \left[ \vec{S}_1 \cdot (\vec{r} \times \vec{v}) \right] \right. \\ \left. + 4(42m_1 + 19m_2) n^i (\hat{n} \cdot \vec{v}) \left( \vec{S}_1 \times \vec{r} \right)^j \right. \\ \left. - 4(32m_1 + 7m_2) r^i \left( \vec{S}_1 \times \vec{v} \right)^j - 2(12m_1 + 13m_2) v^i \left( \vec{S}_1 \times \vec{r} \right)^j \right\} \mathcal{E}_{ij}. \quad (65)$$

For the radiative processes with magnetic parity one has

$$L_{fig.16} = 768 \frac{G_N^2 m_2}{r^2 (\tilde{\Lambda}r)^6} \left[ - (3m_1 + 5m_2) S_1^i r^j + 2(9m_1 + 4m_2) n^i n^j \left( \vec{S}_1 \cdot \vec{r} \right) \right] \mathcal{B}_{ij}. \quad (66)$$

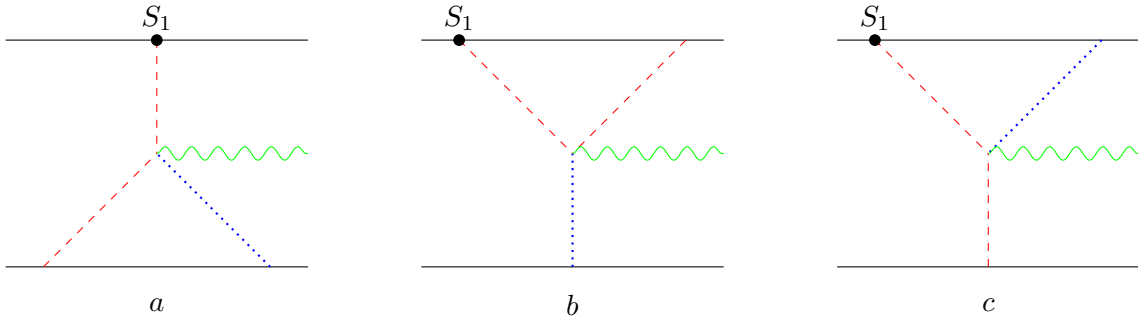


Figure 15: Diagrams representing the correction to the linear-in-spin *electric* radiation emission mediated by the  $\tilde{\mathcal{C}}^2$  bulk interaction. Diagrams must be supplemented with their mirror images under  $1 \leftrightarrow 2$ .

## IV. DISCUSSION

Following the parameterisation of short-distance gravity modification introduced in [6], we applied effective field theory methods of non-relativistic General Relativity [7] to preliminarily re-derive in this modified gravity model the energy and luminosity functions of a compact two-body system for non-spinning systems, which are the ingredients to compute the phase

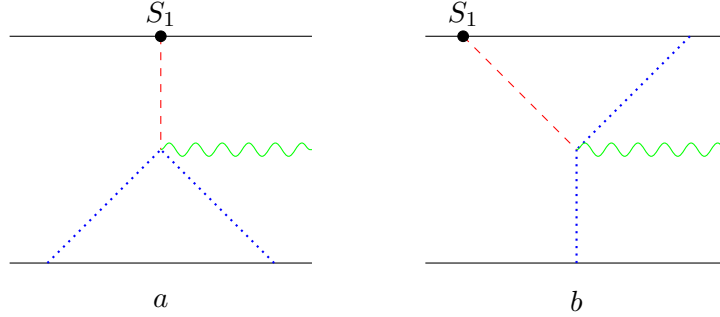


Figure 16: Diagrams representing the correction to the linear-in-spin *magnetic* radiation emission mediated by the  $\tilde{\mathcal{C}}^2$  bulk interaction. Diagrams must be supplemented with their mirror images under  $1 \leftrightarrow 2$ .

of gravitational waves observed routinely since the year 2015 by the gravitational wave observatories LIGO and Virgo. Moreover, applying standard treatment of spin degrees of freedom, we have extended these results to the linear-in-spin case, with the new result of deriving linear-in-spin potentials, radiative terms and spin precessing equations from the same modifications to General Relativity, hence adding a new test of General Relativity. Another new finding of the present work is given by corrections to the quadrupole formula that must be included into emission processes and luminosity functions when dealing with General Relativity modifications altering the equation of motion of the sources, as explained in sec. III A 2.

However, irrespectively of physical quantities being considered (2-body potential, luminosity, gravitational wave phasing, spin equation of motion), the corrections due to the quartic interactions introduced by the extra terms of the type Riemann to the fourth power can be classified as 2PN order in the post-Newtonian approximation ( $n$ PN meaning  $v^{2n}$  corrections with respect to leading order) times a factor  $(\Lambda r)^{-6}$  (being  $\Lambda$  the generic short-distance scale introduced by the quartic curvature terms and  $r$  the typical source size) with respect to leading order for parity (and time-reversal) preserving interactions, and 1.5 PN (again times  $(\Lambda r)^{-6}$ ) for parity-violating corrections for both spinning and non-spinning systems.

For spins however, we have to consider that in General Relativity the leading spin-dependent term in the gravitational wave phasing formula appears at 1.5PN order, and the quartic curvature interactions considered in this work give a 1.5PN (as it happens in the

parity-violating case, or 2PN in the parity preserving one) correction with respect to the leading spin order, hence 3PN (3.5PN) order in absolute terms, times the usual  $(\Lambda_{-}r)^{-6}$  or  $(\Lambda r)^{-6}$  factor.

Current limits set by LIGO/Virgo detections on 2PN and 3PN phasing terms [29, 30] require them to be within  $\sim 10\%$  of the value predicted by General Relativity, giving a mild bound on  $\Lambda \gtrsim 1/r$ , with typical  $r$  for LIGO/Virgo detections of the order of  $\sim 10 - 100$  km, which translated to an energy scale is  $\Lambda \gtrsim 10^{-12,-13}$  eV, see [31] for a Bayesian model selection approach used on two real gravitational wave events and [32] for the geometry of single black hole solutions. Note that while the bound that can be set with this type of analysis are rather loose, we have provided in this work a first *ab initio* computation of spin effects in two body potential, emission and spin precession equations.

Other tests are possible via *geodetic precession*, i.e. relativistic spin precession which in General Relativity is caused at leading order by the spin-orbit coupling, that has been observed in the spin of double pulsar PSR J0737-3039 [33–35] and it is currently in agreement with the value predicted by General Relativity at 13% level.

For the gravitational model under study here, parity-preserving terms give rise to corrections of the order  $v^4 \times (\Lambda r)^{-6}$  to the spin precessing equations, as reported in eqs. (45) and (64). Using the value of orbital velocity of the double pulsar  $v \sim 10^{-3}$ , geodetic precession gives a weaker constraint on  $\Lambda, \tilde{\Lambda}$  ( $\Lambda \gtrsim 10^{-17}$  eV) than the one from GW phasing because of the larger size of the binary pulsars systems ( $r \sim 10^6$  km) with respect to typical GW coalescing binary sources. Considering the bounds from Gravity Probe B [36], which constrained the geodetic precession with 1% precession, the relevant velocity and system size being  $v \sim 3 \times 10^{-5}$  and  $r \sim 4000$  km, one obtains  $\Lambda \gtrsim 10^{-16}$  eV.

Note however the presence in the spin precession equation (56) of a term  $\sim \vec{r} \times \vec{S}_1$ , being  $\vec{r}$  the orbital radius vector, at  $1.5\text{PN} \times (\Lambda_{-}r)^{-6}$  level in the parity violating case. Such term induces an oscillation at the orbital frequency  $\sim v/r$  on the top of the leading precession effect which has frequency  $v^3/r$ , see eq. (29). In General Relativity the spin equations of motion at next-to-leading order have a term quadratic in the  $\vec{r}$  vector which can produce nutation of the spin at twice the orbital frequency [37], but the presence of a modulation at the orbital frequency in the spin precession equation would be a smoking gun of the parity violating term  $\vec{r} \times \vec{S}_1$ . The magnitude of this effect is suppressed by  $v^3 \times (\Lambda_{-}r)^{-6}$  with respect to the leading order precession equation, hence assuming  $N$  orbital cycles of

observations, one would get the limit  $\Lambda_- \gtrsim 10^{-16, -15} \text{eV} \times N^{1/12}$  for the double pulsar and Gravity Probe B respectively, which can observe  $10^{3,4}$  orbital cycles per year.

Overall, we have extended the analysis of [6] on the effect that high curvature terms have on binary systems to include linear-in-spin effects in energy, radiation emission and the spin precession equations, the last being an important test-bed of gravity for spinning systems.

### Acknowledgements

The authors wish to thank Shao Lijing for useful correspondence. The work of ANL is financed in part by the Coordenação de Aperfeiçoamento de Pessoal de Nível Superior - Brasil (CAPES) - Finance Code 001. RS is partially supported by CNPq. RS would like to thank ICTP-SAIFR FAPESP grant 2016/01343-7.

### Appendix A: Derivation of multipolar radiative coupling in GR

The first diagram in fig. 2 can be read directly from the Lagrangian (6), the second one needs the  $\phi^2\sigma$  Lagrangian bulk term which appears in eq. (4)

$$L_{rad-2b} = \frac{m_1 m_2}{8m_{Pl}^2} \int \frac{d^3k}{(2\pi)^3} \frac{k^i k^j}{k^4} e^{i\vec{k}\cdot\vec{r}} = -\frac{G_N m_1 m_2 r^i r^j}{2r^3} \frac{\sigma_{ij}}{m_{Pl}}, \quad (\text{A1})$$

where a term proportional to the trace of  $\sigma$  has been neglected, since it does not contribute to radiation in the TT gauge. Using trivial identities and  $m_1 \ddot{x}_1 + m_2 \ddot{x}_2 = 0$ , which is valid in general, not only in GR, one can rewrite the radiative coupling as

$$\begin{aligned} L_{rad-LO} &= m_1 \left( v_1^i v_1^j - \frac{G_N m_2}{2r^3} r^i r^j \right) \frac{\sigma_{ij}}{2m_{Pl}} + 1 \leftrightarrow 2 \\ &= m_1 \left[ v_1^i v_1^j + \frac{1}{2} \ddot{x}_1^i (x_1^j - x_2^j) - \frac{r^j}{2} \left( \frac{G_N m_2}{r^3} r^i + \ddot{x}_1^i \right) \right] \frac{\sigma_{ij}}{2m_{Pl}} + 1 \leftrightarrow 2 \\ &= \left[ m_1 v_1^i v_1^j + \frac{m_1}{2} \ddot{x}_1^i x_1^j + \frac{m_2}{2} \ddot{x}_2^i x_2^j - \frac{m_1}{2} r^i \left( \frac{G_N m_2}{r^3} r^j + \ddot{x}_1^j \right) \right] \frac{\sigma_{ij}}{2m_{Pl}} + 1 \leftrightarrow 2 \\ &= \left[ \frac{m_1}{2} \frac{d^2}{dt^2} (x_1^i x_1^j) + \frac{m_2}{2} \frac{d^2}{dt^2} (x_2^i x_2^j) - r^i \left( \frac{G_N m_1 m_2}{r^3} r^j + \frac{m_1}{2} \ddot{x}_1^j - \frac{m_2}{2} \ddot{x}_2^j \right) \right] \frac{\sigma_{ij}}{2m_{Pl}}, \end{aligned} \quad (\text{A2})$$

which shows explicitly that the standard GR result (11) is recovered on the equations of motions, but it also shows that in the case of modified equations of motion, for which e.g.  $\ddot{x}_1^i = -G m_2 r^i (1 + O(\Lambda r)^{-6})$ , extra terms appear in the radiative coupling.

The usual textbook procedure to derive the source multipole coupling to radiation is equivalent for the mass quadrupole to the explicit calculation (A2) in GR, but it does not

take account GR deviations, and for an extended source (like a binary system, extended over a volume  $V$ ) whose size  $r \ll \lambda_{gw}$ , being  $\lambda_{gw}$  the GW wavelength, goes as follows:

$$\begin{aligned} \mathcal{S}_{mult} &= \frac{1}{2} \int dt \int d^3x T^{\mu\nu}(t, \vec{x}) h_{\mu\nu}(t, \vec{x}) \simeq \\ & \frac{1}{2} \int dt \left\{ \left( \int_V T^{00} \right) h_{00} + \left[ 2 \left( \int_V T_{0i} \right) h_{0i} + \left( \int_V T^{00} x^i \right) h_{00,i} \right] + \right. \\ & \left[ \left( \int_V T^{ij} \right) h_{ij} + \left( \int_V T_{0i,j} \right) (h_{0i,j} + h_{0j,i}) + \frac{1}{2} \left( \int_V T_{00} x^i x^j \right) h_{00,ij} \right] \\ & \left. + \left( \int_V T_{0i,j} \right) (h_{0i,j} - h_{0j,i}) + \left( \int_V T^{ij} x^k \right) h_{ij,k} + \dots \right\}, \end{aligned} \quad (\text{A3})$$

where the notation  $\int_V = \int d^3x$  has been adopted for brevity and all gravitational fields  $h$  and their derivatives have to be computed at  $\vec{x} = 0$ . Note that this Taylor expansion is actually an expansion in  $r/\lambda_{gw} \sim v$  where  $v$  is the source internal velocity.

Using repeatedly the energy-momentum conservation in the form  $\dot{T}^{\mu 0} = -T^{\mu i}{}_{,i}$  one can derive

$$\begin{aligned} \int_V T^{ij} &= \frac{1}{2} \frac{d^2}{dt^2} \left( \int_V T^{00} x^i x^j \right) \equiv \frac{1}{2} \ddot{Q}^{ij}, \\ \int_V T^{0i} &= -\frac{d}{dt} \left( \int_V T^{00} x^i \right), \\ \int_V T^{ij} x^k &= \frac{1}{3} \int_V (T^{ij} x^k + T^{ki} x^j + T^{jk} x^i) + \frac{1}{3} \int_V (2T^{ij} x^k - T^{ik} x^j - T^{jk} x^i), \\ &= \frac{1}{6} \frac{d^2}{dt^2} \left( \int_V T^{00} x^i x^j x^k \right) + \frac{1}{3} \frac{d}{dt} \left[ \int_V (T^{0i} x^k x^j + T^{0j} x^k x^i - 2T^{0k} x^i x^j) \right], \end{aligned} \quad (\text{A4})$$

The coupling  $T^{ij} h_{ij}$  hence gives rise to the electric quadrupole coupling  $\frac{1}{2} Q^{ij} R_{0i0j}$  term, where the linear order expression of  $R_{0i0j}$  in terms of the Kaluza-Klein fields  $\phi, A_i, \sigma_{ij}$  is given in eq. (12).

Moreover defining

$$\begin{aligned} O^{ijk} &\equiv \int_V T^{00} x^i x^j x^k, \\ J^{ij} &\equiv \frac{1}{2} \int_V T^0_l x_k (x^i \epsilon^{jkl} + x^j \epsilon^{ikl}), \end{aligned} \quad (\text{A5})$$

using the identity

$$\begin{aligned} (T^{0i} x^k x^j - T^{0k} x^i x^j) \sigma_{ij,k} &= T^{0m} x^n x^j (\delta_m^l \delta_n^k - \delta_m^k \delta_n^l) \sigma_{lj,k} \\ &= \epsilon_{imn} T^{0m} x^n x^j \frac{1}{2} \epsilon^{ikl} (\sigma_{jk,l} - \sigma_{jl,k}), \end{aligned} \quad (\text{A6})$$

and the definition of the magnetic part of the Riemann tensor

$$\mathcal{B}_{ij} \equiv \frac{1}{2} \epsilon_{ikl} R_{0jkl} \simeq \frac{1}{4m_{Pl}} \epsilon_{ikl} \left[ \dot{\sigma}_{jk,l} - \dot{\sigma}_{jl,k} + A_{l,jk} - A_{k,jl} + \frac{1}{d-2} (\dot{\phi}_{,k} \delta_{jl} - \dot{\phi}_{,l} \delta_{jk}) \right], \quad (\text{A7})$$

one finds explicitly the magnetic and electric quadrupole and electric octupole gravitational couplings of eq. (14), with  $J_{ij} = T^{0m} x^n (\epsilon_{imn} x_j + \epsilon_{jmn} x_i) / 2$ .

At the next order in eq. (A3), i.e electric exadecapole and magnetic octupole, one has the following identity, see [38] for an explicit Lagrangian treatment or [15] for general derivation of the multipole expansion,

$$\begin{aligned} \frac{1}{4} \int_V T^{ij} x^k x^l &= \frac{1}{4} \times \frac{1}{6} \int_V (T^{ij} x^k x^l + T^{li} x^j x^k + T^{kl} x^i x^j + T^{jk} x^l x^i + T^{ik} x^j x^l + T^{jl} x^i x^k) \\ &+ \frac{1}{4} \times \frac{1}{2} \int_V (T^{ij} x^k x^l - T^{kl} x^i x^j) \\ &+ \frac{1}{4} \times \frac{1}{6} \int_V (2T^{ij} x^k x^l + 2T^{kl} x^i x^j - T^{li} x^j x^k - T^{jk} x^l x^i - T^{ik} x^j x^l - T^{jl} x^i x^k), \end{aligned} \quad (\text{A8})$$

where the first line contains the electric exadecapole  $l = 4$ , the second line contains the magnetic octupole  $l = 3$  and the third line is a contribution to the electric quadrupole ( $l = 2$ ). From the third line of (A8) one gets the multipole coupling

$$\begin{aligned} &\frac{1}{4} \left( \int_V T^{ij} x^k x^l \right) \Big|_{(\text{A8})3rd\ line} \sigma_{ij,kl} \\ &= \frac{1}{12} \left( \int_V T^{ij} x^k x^l \right) (\sigma_{ij,kl} + \sigma_{kl,ij} - \sigma_{il,jk} - \sigma_{jk,il}) \\ &= -\frac{1}{12} \epsilon_{ikm} \epsilon_{jln} \left( \int_V T^{ij} x^k x^l \right) \frac{\ddot{\sigma}^{mn}}{m_{Pl}} \\ &= \frac{1}{12} \left( \int_V T^{ll} x^m x^n + T^{mn} r^2 - T^{ml} x^n x^l - T^{nl} x^l x^m \right) \frac{\ddot{\sigma}^{mn}}{m_{Pl}}, \end{aligned} \quad (\text{A9})$$

where the relationships

$$R_{ijkl} = -\epsilon_{ijm} \epsilon_{klm} R_{0m0n}, \quad (\text{A10})$$

$$R_{ijkl} = \frac{1}{2} (\sigma_{il,jk} + \sigma_{jk,il} - \sigma_{ik,jl} - \sigma_{jl,ik}) + O(\sigma^2), \quad (\text{A11})$$

have been used, which are valid for the radiative field. To collect all the electric quadrupole contributions from second order multipole expansions one must add to eq. (A9) the terms obtained by subtracting traces from the first and second line of (A8):

$$\begin{aligned} \frac{1}{4} \left( \int_V T^{ij} x^k x^l \right) \Big|_{Tr-Exa} \sigma_{ij,kl} &= \frac{1}{4} \times \frac{1}{42} \int_V (T^{ij} r^2 + T^{ll} x^i x^j + 2(T^{il} x^l x^j + T^{jl} x^l x^i)) \ddot{\sigma}_{ij}, \\ \frac{1}{4} \left( \int_V T^{ij} x^k x^l \right) \Big|_{Tr-Oct} \sigma_{ij,kl} &= -\frac{1}{4} \times \frac{1}{6} \int_V (T^{ll} x^i x^j - T^{ij} r^2) \ddot{\sigma}_{ij}, \end{aligned} \quad (\text{A12})$$

where we used that the gravitational field is on-shell and in vacuum (i.e.  $\ddot{\sigma}_{ij} = \nabla^2 \sigma_{ij}$  and  $\sigma_{ij,j} = 0$ ).

In the standard approach one then uses repeatedly the energy momentum conservation equation to derive

$$\begin{aligned}
\int_V (T^{ij} r^2 + T^{ll} x^i x^j) &= \int_V \left[ \left( -\frac{1}{2} \ddot{T}^{00} r^2 + 2 \dot{T}^{0l} x^l \right) x^i x^j + \left( \dot{T}^{i0} x^j + \dot{T}^{j0} x^i \right) r^2 \right. \\
&\quad \left. - 2 (T^{im} x^m x^j + T^{jm} x^m x^i) \right], \\
\int_V (T^{il} x^l x^j + T^{jl} x^l x^i) &= \int_V \left[ \left( \dot{T}^{0l} x^l - T^{ll} \right) x^i x^j \right], \\
\int_V \left( \dot{T}^{i0} x^j + \dot{T}^{j0} x^i \right) r^2 &= \int_V \left( \ddot{T}^{00} r^2 x^i x^j - 2 \dot{T}^{0l} x^l x^i x^j \right),
\end{aligned} \tag{A13}$$

from which one recovers the standard form of the radiative electric quadrupole involved in the GR electric quadrupole coupling (11) (valid up to  $O(v^2)$  with respect to LO)

$$-\frac{1}{2} I^{ij} R_{0i0j} = -\frac{1}{2} R_{0i0j} \int_V \left( T^{00} + T^{ll} - \frac{4}{3} \dot{T}^{0l} x^l + \frac{11}{42} \ddot{T}^{00} r^2 \right) x^i x^j. \tag{A14}$$

However since we are using non-GR equation of motions to derive the main results of this paper, in particular in secs. III A 2, III B 2 and III C 2, we will use the GR-equivalent multipole expanded coupling (A3)

$$\begin{aligned}
&\frac{1}{2} \int_V T^{ij}(t, \vec{x}) \frac{\sigma_{ij}(t, \vec{x})}{m_{Pl}} \\
&\simeq \frac{\sigma_{ij}(t, 0)}{2m_{Pl}} \int_V \left[ T^{ij} + \frac{1}{7} \frac{d^2}{dt^2} \left( \frac{2}{3} T^{ll} x^i x^j + \frac{11}{6} T^{ij} r^2 - T^{il} x^l x^j - T^{jl} x^l x^i \right) \right].
\end{aligned} \tag{A15}$$

One can check explicitly that eqs. (A14) and (A15) are equivalent in GR on the equation of motions, in particular for the spinning case by using in eq. (A15) the energy momentum tensor  $T_{ij}$  derived via the sum of eqs. (33) and (34), the equation of motion (30) and (A2). In eq. (A14) the LO part of  $T^{00}$ ,  $T^{0i}$  and electric part of  $T^{ij}$  can be read directly from the point-particle Lagrangian (24). In the right hand side of eq. (A15) the LO part of  $T^{ij}$  does not contribute to the electric coupling in the first term (the one without time derivatives), but it does in the terms involving two time derivatives.



## Appendix B: Higher order curvature contributions to the conservative Lagrangian

### 1. No Spin

#### a. $\mathcal{C}^2$

The amplitudes corresponding to the diagrams in fig. 5 are

$$\begin{aligned}
 A_{fig. 5a} &= i \frac{m_1 m_2^3}{8m_{Pl}^6 \Lambda^6} \int_{\mathbf{p}, \mathbf{k}_1, \mathbf{k}_2} e^{i\vec{p}\cdot\vec{r}} \frac{[\vec{k}_2 \cdot (\vec{k}_1 - \vec{k}_2)]^2 [\vec{p} \cdot (\vec{p} - \vec{k}_1)]^2}{p^2 (p - k_1)^2 (k_1 - k_2)^2 k_2^2} = -i512 \frac{G_N^3 m_1 m_2^3}{\Lambda^6 r^9}, \\
 A_{fig. 5b} &= i \frac{m_1^2 m_2^2}{16m_{Pl}^6 \Lambda^6} \int_{\mathbf{p}, \mathbf{k}_1, \mathbf{k}_2} e^{i\vec{p}\cdot\vec{r}} \times \\
 &\quad \frac{[\vec{k}_1 \cdot (\vec{p} - \vec{k}_1)]^2 [\vec{k}_2 \cdot (\vec{p} - \vec{k}_2)]^2 + 2 (\vec{k}_1 \cdot \vec{k}_2)^2 [(\vec{p} - \vec{k}_1) \cdot (\vec{p} - \vec{k}_2)]^2}{(\vec{p} - \vec{k}_1)^2 \vec{k}_1^2 (\vec{p} - \vec{k}_2)^2 \vec{k}_2^2} = 0,
 \end{aligned} \tag{B1}$$

giving the result of eq. (41). They can be computed by repeated use (and differentiations) of the standard 1-loop master integral

$$\int_{\mathbf{k}} \frac{1}{k^{2a} (p - k)^{2b}} = \frac{(p^2)^{d/2-2}}{(4\pi)^{d/2}} \frac{\Gamma(d/2 - a)\Gamma(d/2 - b)\Gamma(a + b - d/2)}{\Gamma(a)\Gamma(b)\Gamma(d - a - b)}, \tag{B2}$$

and of the fundamental integral

$$\int_{\mathbf{p}} \frac{e^{i\vec{p}\cdot\vec{r}}}{p^{2a}} = \frac{1}{2^{2a} \pi^{d/2}} \frac{\Gamma(d/2 - a)}{\Gamma(a)} r^{2a-d}. \tag{B3}$$

## 2. Spin

### a. $\mathcal{C}^2$

The amplitudes from diagrams in fig. 6, grouped according to the gravitational polarisation attached to the spin, are the following:

$$\begin{aligned}
A_{fig.6-A} &= -\frac{m_1^2 m_2}{8m_{Pl}^6 \Lambda^6} \int_{\mathbf{p}, \mathbf{k}_1, \mathbf{k}_2} \frac{e^{i\vec{p}\cdot\vec{r}}}{p^2 (p-k_1)^2 (k_1-k_2)^2 k_2^2} \times \left( \vec{k}_2 \cdot \vec{v}_1 \right) \\
&\quad \times \left\{ \left[ \vec{p} \cdot (\vec{p} - \vec{k}_1) \right]^2 \left( \vec{k}_1 - \vec{k}_2 \right) \cdot \vec{k}_2 (k_1 - k_2)^j \right. \\
&\quad \left. + \left[ \left( \vec{k}_1 - \vec{k}_2 \right) \cdot (\vec{p} - \vec{k}_1) \right]^2 \vec{p} \cdot \vec{k}_2 \frac{1}{2} p^j \right\} k_2^i S_{1ij} \\
&= i \frac{1152 G_N^3 m_1^2 m_2}{(\Lambda r)^6 r^5} r_i v_{1j} S_1^{ij}, \\
A_{fig.6-\phi} &= -\frac{m_2}{8m_{Pl}^6 \Lambda^6} \int_{\mathbf{p}, \mathbf{k}_1, \mathbf{k}_2} \frac{e^{i\vec{p}\cdot\vec{r}}}{p^2 (p-k_1)^2 (k_1-k_2)^2 k_2^2} \\
&\quad \times \left\{ m_1^2 \left\{ 2 \left[ \left( \vec{k}_1 - \vec{k}_2 \right) \cdot \vec{k}_2 \right]^2 \left[ \vec{p} \cdot (\vec{p} - \vec{k}_1) \right]^2 \right. \right. \\
&\quad \left. \left. + \left[ \left( \vec{k}_1 - \vec{k}_2 \right) \cdot (\vec{p} - \vec{k}_1) \right]^2 \left[ \vec{p} \cdot \vec{k}_2 \right]^2 \right\} \right. \\
&\quad \left. - m_2^2 \left\{ \vec{p} \cdot (\vec{p} - \vec{k}_1) \right\}^2 \left[ \vec{k}_2 \cdot (\vec{k}_1 - \vec{k}_2) \right]^2 \right\} p_i (S_1^{i0} + v_{1j} S_1^{ij}) \\
&= i \frac{4608 G_N^3 m_2}{(\Lambda r)^6 r^5} (m_1^2 + m_2^2) (r_i S_1^{i0} + r_i v_{1j} S_1^{ij}), \\
A_{fig.6-\sigma} &= \frac{m_1^2 m_2}{16m_{Pl}^6 \Lambda^6} \int_{\mathbf{p}, \mathbf{k}_1, \mathbf{k}_2} \frac{e^{i\vec{p}\cdot\vec{r}}}{p^2 (p-k_1)^2 (k_1-k_2)^2 k_2^2} \left\{ \left[ \left( \vec{k}_1 - \vec{k}_2 \right) \cdot (\vec{p} - \vec{k}_1) \right]^2 \vec{p} \cdot \vec{k}_2 p^j \right. \\
&\quad \left. + 2 \left[ \vec{p} \cdot (\vec{p} - \vec{k}_1) \right]^2 \left( \vec{k}_1 - \vec{k}_2 \right) \cdot \vec{k}_2 (k_1 - k_2)^j \right\} \vec{k}_2 \cdot \vec{v}_1 k_2^i S_{1ij} \\
&= -i \frac{1152 G_N^3 m_1^2 m_2}{(\Lambda r)^6 r^5} r_i v_{1j} S_1^{ij},
\end{aligned} \tag{B4}$$

which add up to give the potential

$$V_{\Lambda S_1} = -\frac{4608 G_N^3 m_2}{(\Lambda r)^6 r^5} (m_1^2 + m_2^2) (r_i S_1^{i0} + r_i v_{1j} S_1^{ij}), \tag{B5}$$

leading via eq. (26) to eq. (45).

b.  $\mathcal{C}\tilde{\mathcal{C}}$ 

The amplitudes from diagrams in fig. 10 are

$$\begin{aligned}
A_{fig.10a} &= -\frac{m_1^2 m_2}{4m_{Pl}^6 \Lambda_-^6} \int_{\mathbf{p}, \mathbf{k}_1, \mathbf{k}_2} \frac{e^{i\vec{p}\cdot\vec{r}} (p-k_1)^l}{p^2 (p-k_1)^2 (k_1-k_2)^2 k_2^2} \left\{ \left[ (\vec{k}_1 - \vec{k}_2) \cdot \vec{k}_2 \right]^2 \left[ \vec{p} \cdot (\vec{p} - \vec{k}_1) \right] p^j \right. \\
&\quad \left. + 2 \left[ \vec{p} \cdot \vec{k}_2 \right]^2 \left[ (\vec{p} - \vec{k}_1) \cdot (\vec{k}_1 - \vec{k}_2) \right] (k_1 - k_2)^j \right\} (p-k_1)^k \epsilon_{ijk} S_1^{il} \\
&= i \frac{2304}{(\Lambda_- r)^6} \frac{G_N^3 m_1^2 m_2}{r^5} \epsilon_{ijk} r^i S_1^{jk}, \\
A_{fig.10b} &= \frac{m_2^3}{8m_{Pl}^6 \Lambda_-^6} \int_{\mathbf{p}, \mathbf{k}_1, \mathbf{k}_2} \frac{e^{i\vec{p}\cdot\vec{r}}}{p^2 (p-k_1)^2 (k_1-k_2)^2 k_2^2} \\
&\quad \times \left[ (\vec{k}_1 - \vec{k}_2) \cdot \vec{k}_2 \right]^2 \left[ \vec{p} \cdot (\vec{p} - \vec{k}_1) \right] p^l k_1^j p^k \epsilon_{ijk} S_1^{il} = 0, \\
A_{fig.10c} &= \frac{m_1 m_2^2}{8m_{Pl}^6 \Lambda_-^6} \int_{\mathbf{p}, \mathbf{k}_1, \mathbf{k}_2} \frac{e^{i\vec{p}\cdot\vec{r}}}{(p-k_1)^2 k_1^2 (p-k_2)^2 k_2^2} \\
&\quad \times \left\{ \left[ \vec{k}_2 \cdot (\vec{p} - \vec{k}_2) \right]^2 \left[ (\vec{p} - \vec{k}_1) \cdot \vec{k}_1 \right] k_1^j p^k \right. \\
&\quad \left. + \left( \vec{k}_1 \cdot \vec{k}_2 \right)^2 \left[ (\vec{p} - \vec{k}_1) \cdot \vec{k}_2 \right] (p-k_2)^j (p-k_2)^k \right\} \left( \vec{p} - \vec{k}_1 \right)^l \epsilon_{ijk} S_1^{il} = 0,
\end{aligned} \tag{B6}$$

giving the potential in eq. (55).

c.  $\tilde{\mathcal{C}}^2$ 

The amplitudes from the non-vanishing diagrams in fig. 14 are

$$\begin{aligned}
A_{fig.14d} &= -\frac{2m_1^2 m_2}{m_{Pl}^6 \tilde{\Lambda}^6} \int_{\mathbf{p}, \mathbf{k}_1, \mathbf{k}_2} \frac{e^{i\vec{p}\cdot\vec{r}}}{p^2 (p-k_1)^2 (k_1-k_2)^2 k_2^2} \\
&\quad \times \left\{ \left[ (\vec{p} - \vec{k}_1) \cdot \vec{k}_2 \right] \left[ \vec{p} \cdot (\vec{k}_1 - \vec{k}_2) \right] k_2^k p^n + \left[ (\vec{p} - \vec{k}_1) \cdot \vec{p} \right] \left[ \vec{k}_2 \cdot (\vec{k}_1 - \vec{k}_2) \right] p^k k_2^n \right\} \\
&\quad \times (p-k_1)^i (p-k_1)^l v_1^m (k_1-k_2)^r \epsilon_{jkl} \epsilon_{mnr} S_1^{ij} \\
&= i \frac{55296}{11(\tilde{\Lambda}r)^6} \frac{G_N^3 m_1^2 m_2}{r^5} r^i v_1^j S_{1ij}, \\
A_{fig.14e} &= -\frac{2m_1^2 m_2}{m_{Pl}^6 \tilde{\Lambda}^6} \int_{\mathbf{p}, \mathbf{k}_1, \mathbf{k}_2} \frac{e^{i\vec{p}\cdot\vec{r}} \left[ \vec{p} \cdot (\vec{k}_1 - \vec{k}_2) \right] \left[ (\vec{p} - \vec{k}_1) \cdot \vec{k}_2 \right]}{p^2 (p-k_1)^2 (k_1-k_2)^2 k_2^2} \\
&\quad \times (p-k_1)^i k_2^k (p-k_1)^l v_2^m (k_1-k_2)^n p^r \epsilon_{jkl} \epsilon_{mnr} S_1^{ij} \\
&= -i \frac{55296}{11(\tilde{\Lambda}r)^6} \frac{G_N^3 m_1^2 m_2}{r^5} r^i v_2^j S_{1ij},
\end{aligned} \tag{B7}$$

whose sum gives eq. (63).

## Appendix C: Higher order curvature contributions to radiative coupling

### 1. No spin

#### a. $\mathcal{C}^2$

The leading correction to radiative coupling is given by the diagram in fig. 7 resulting in amplitudes

$$\begin{aligned}
 A_{fig. 7} &= i \frac{m_1 m_2}{m_{Pl}^4 \Lambda^6} \int_{\mathbf{p}, \mathbf{k}} e^{i\vec{p}\cdot\vec{r}} \frac{p^i p^j \left[ \vec{k} \cdot (\vec{p} - \vec{k}) \right]^2 + 2k^i k^j \left[ \vec{p} \cdot (\vec{p} - \vec{k}) \right]^2}{p^2 (p-k)^2 k^2} \times R_{0i0j} \\
 &= i 1344 \frac{G_N^2 m_1 m_2}{(\Lambda r)^6} n^i n^j R_{0i0j},
 \end{aligned} \tag{C1}$$

to which the diagrams obtained under 1  $\leftrightarrow$  2 exchange must be added, and terms  $\propto \delta^{ij} R_{0i0j}$  which are vanishing on-shell have been neglected. This amplitude is needed to arrive at eq. (46).

#### b. $\mathcal{C}\tilde{\mathcal{C}}$

The diagram in figs.11 are worth the following amplitudes

$$\begin{aligned}
 A_{fig.11a} &= -i \frac{m_1 m_2}{m_{Pl}^4 \tilde{\Lambda}^6} \int_{\mathbf{p}, \mathbf{k}} \frac{e^{i\vec{p}\cdot\vec{r}}}{p^2 (p-k)^2 k^2} \left\{ p^i p^j \left[ \vec{k} \cdot (\vec{p} - \vec{k}) \right]^2 + 2k^i k^j \left[ \vec{p} \cdot (\vec{p} - \vec{k}) \right]^2 \right\} \mathcal{B}_{ij} \\
 &= -i \frac{1344}{(\tilde{\Lambda} r)^6} \frac{G_N^2 m_1 m_2}{r^2} r^i r^j \mathcal{B}_{ij}, \\
 A_{fig.11b} &= i \frac{2m_1 m_2}{m_{Pl}^4 \tilde{\Lambda}^6} \int_{\mathbf{p}, \mathbf{k}} \frac{e^{i\vec{p}\cdot\vec{r}}}{p^2 (p-k)^2 k^2} \left[ (\vec{k} \cdot \vec{p})^2 + p^4 - 2p^2 (\vec{p} \cdot \vec{k}) \right] k^i k^k v_2^l \epsilon_{ijkl} R_{0i0j} \\
 &= -i \frac{1152}{(\tilde{\Lambda} r)^6} \frac{G_N^2 m_1 m_2}{r^2} r^i r^k v_2^l \epsilon_{ijkl} \mathcal{E}_{ij}, \\
 A_{fig.11c} &= i \frac{2m_1 m_2}{m_{Pl}^4 \tilde{\Lambda}^6} \int_{\mathbf{p}, \mathbf{k}} \frac{e^{i\vec{p}\cdot\vec{r}}}{p^2 (p-k)^2 k^2} \left[ (\vec{k} \cdot \vec{p})^2 + k^4 - 2k^2 (\vec{p} \cdot \vec{k}) \right] p^i p^k v_1^l \epsilon_{ijkl} R_{0i0j} \\
 &= -i \frac{1536}{(\tilde{\Lambda} r)^6} \frac{G_N^2 m_1 m_2}{r^2} r^i r^k v_1^l \epsilon_{ijkl} \mathcal{E}_{ij},
 \end{aligned} \tag{C2}$$

from which eqs.(57) and (59) follow.

## 2. Spin

### a. $C^2$

The leading, linear-in-spin corrections to the magnetic quadrupole comes from diagrams in fig. 8, whose amplitudes are respectively for the magnetic case

$$\begin{aligned}
A_{fig.8a} &= \frac{2m_1m_2}{m_{Pl}^4\Lambda^6} \int_{\mathbf{p},\mathbf{k}} e^{i\vec{p}\cdot\vec{r}} \frac{[\vec{p}\cdot(p-k)]^2}{p^2(p-k)^2k^2} k^i \left[ S_1^j k^2 - k^j (\vec{k}\cdot\vec{S}_1) \right] \mathcal{B}_{ij} \\
&= i768 \frac{G_N^2 m_1 m_2}{\Lambda^6 r^8} \left[ 2r^i S_1^j - 5n^i n^j (\vec{r}\cdot\vec{S}_1) \right] \mathcal{B}_{ij}, \\
A_{fig.8b} &= i \frac{m_2^2}{m_{Pl}^4\Lambda^6} \int_{\mathbf{p},\mathbf{k}} e^{i\vec{p}\cdot\vec{r}} \frac{[\vec{k}\cdot(p-k)]^2}{p^2(p-k)^2k^2} p^i \left[ S_1^j \vec{p}\cdot(\vec{p}-\vec{k}) - (p-k)^j (\vec{p}\cdot\vec{S}_1) \right] \mathcal{B}_{ij} \\
&= i384 \frac{G_N^2 m_2^2}{\Lambda^6 r^8} \left( 5r^i S_1^j - 8n^i n^j (\vec{r}\cdot\vec{S}_1) \right) \mathcal{B}_{ij},
\end{aligned} \tag{C3}$$

whose sum reproduces eq. (48).

The leading, linear-in-spin electric quadrupole corrections are due to the diagrams in fig. 9 which give:

$$\begin{aligned}
A_{fig.9a} &= -i \frac{m_2^2}{4m_{Pl}^4\Lambda^6} \int_{\mathbf{p},\mathbf{k}} e^{i\vec{p}\cdot\vec{r}} \frac{[\vec{k}\cdot(p-k)]^2}{p^2(p-k)^2k^2} [(\vec{p}\cdot\vec{v}_1) p^i - p^2 v_1^i] p^k S_1^{kj} \mathcal{E}_{ij} \\
&= i192 \frac{G_N^2 m_2^2}{\Lambda^6 r^8} \left[ 8(\hat{n}\cdot\vec{v}_1) n^i (\vec{S}_1 \times \vec{r})^j - 4v_1^i (\vec{S}_1 \times \vec{r})^j - r^i (\vec{S}_1 \times \vec{v}_1)^j \right] \mathcal{E}_{ij}, \\
A_{fig.9b} &= i \frac{m_1 m_2}{2m_{Pl}^4\Lambda^6} \int_{\mathbf{p},\mathbf{k}} e^{i\vec{p}\cdot\vec{r}} \frac{[\vec{p}\cdot(p-k)]^2}{p^2(p-k)^2k^2} [(\vec{k}\cdot v_1) k^i - k^2 v_1^i] k^k S_1^{kj} \mathcal{E}_{ij} \\
&= i192 \frac{G_N^2 m_1 m_2}{\Lambda^6 r^8} \left[ 5(\hat{n}\cdot\vec{v}_1) n^i (\vec{S}_1 \times \vec{r})^j - v_1^i (\vec{S}_1 \times \vec{r})^j - r^i (\vec{S}_1 \times \vec{v}_1)^j \right] \mathcal{E}_{ij}, \\
A_{fig.9c} &= i \frac{m_2^2}{m_{Pl}^4\Lambda^6} \int_{\mathbf{p},\mathbf{k}} \frac{e^{i\vec{p}\cdot\vec{r}}}{p^2(p-k)^2k^2} \left\{ [\vec{k}\cdot(\vec{p}-\vec{k})]^2 p^i p^j + 2 [\vec{p}\cdot(\vec{p}-\vec{k})]^2 k^i k^j \right\} \\
&\quad \times (v_1^m S_1^{mn} + S_1^{0n}) \mathcal{E}_{ij} \\
&= -i(1+\kappa) \frac{2688}{(\Lambda r)^6} \frac{G_N m_2^2}{r^2} \left\{ 4n^i n^j [\vec{S}_1 \cdot (\vec{r} \times \vec{v}_1)] + r^i (\vec{S}_1 \times \vec{v}_1)^j \right\} \mathcal{E}_{ij}, \\
A_{fig.9d} &= i \frac{2m_1 m_2}{m_{Pl}^4\Lambda^6} \int_{\mathbf{p},\mathbf{k}} \frac{e^{i\vec{p}\cdot\vec{r}}}{p^2(p-k)^2k^2} \left\{ [\vec{p}\cdot\vec{k}]^2 (p-k)^i (p-k)^j \right. \\
&\quad \left. + [\vec{p}\cdot(\vec{p}-\vec{k})]^2 k^i k^j + [(\vec{p}-\vec{k})\cdot\vec{k}]^2 p^i p^j \right\} k^n (v_1^m S_1^{mn} + S_1^{0n}) \mathcal{E}_{ij} \\
&= -i(1+\kappa) \frac{2688}{(\Lambda r)^6} \frac{G_N m_1 m_2}{r^2} \left\{ 4n^i n^j [\vec{S}_1 \cdot (\vec{r} \times \vec{v}_1)] + r^i (\vec{S}_1 \times \vec{v}_1)^j \right\} \mathcal{E}_{ij},
\end{aligned} \tag{C4}$$

whose sum gives eq. (50).

b.  $\mathcal{C}\tilde{\mathcal{C}}$ 

The diagrams in fig. 12 give the following amplitudes for the electric coupling

$$\begin{aligned}
A_{fig.12\mathcal{E}a} &= i \frac{m_2^2}{m_{Pl}^4 \Lambda_-^6} \int_{\mathbf{p}, \mathbf{k}} \frac{e^{i\vec{p}\cdot\vec{r}} (\vec{p} - \vec{k}) \cdot \vec{k}}{p^2 (p-k)^2 k^2} \\
&\quad \times \left\{ \left[ (\vec{p} - \vec{k}) \cdot \vec{k} \right] p^i \delta^{jm} + 2k^i (p-k)^j k^m \right\} p^r p^k S_{1lr} \epsilon_{jkl} R_{0i0m} \\
&= 1152 \frac{G_N^2 m_2^2}{r^2 (\Lambda_- r)^6} \left[ 5r^i S_1^j - 8n^i n^j (\vec{r} \cdot \vec{S}_1) \right] R_{0i0j}, \\
A_{fig.12\mathcal{E}b} &= i2 \frac{m_1 m_2}{m_{Pl}^4 \Lambda_-^6} \int_{\mathbf{p}, \mathbf{k}} \frac{e^{i\vec{p}\cdot\vec{r}}}{p^2 (p-k)^2 k^2} (p-k)^k (p-k)^r S_{1lr} \epsilon_{jkl} R_{0i0m} \\
&\quad \times \left\{ (\vec{p} \cdot \vec{k})^2 \delta^{jm} (p-k)^i + \left[ (\vec{p} - \vec{k}) \cdot \vec{k} p^i p^m k^j + (\vec{p} - \vec{k}) \cdot \vec{p} k^i k^m p^j \right] \right\} \\
&= 2688 \frac{G_N^2 m_1 m_2}{r^2 (\Lambda_- r)^6} \left[ r^i S_1^j - 4n^i n^j (\vec{r} \cdot \vec{S}_1) \right] R_{0i0j},
\end{aligned} \tag{C5}$$

allowing to derive eq. (61).

For the magnetic coupling one has

$$\begin{aligned}
A_{fig.12Ba} &= 2i \frac{m_2^2}{m_{Pl}^4 \Lambda_-^6} \int_{\mathbf{p}, \mathbf{k}} \frac{e^{i\vec{p}\cdot\vec{r}} \left[ \vec{p} \cdot (\vec{p} - \vec{k}) \right]}{p^2 (p-k)^2 k^2} (\vec{p} \cdot \vec{v}_1) k^i k^j p^k k^l S_{1kl} \mathcal{B}_{ij} \\
&= 384 \frac{G_N^2 m_2^2}{r^2 (\Lambda_- r)^6} \left[ (\vec{r} \times \vec{S}_1)^i v_1^j + (\vec{v}_1 \times \vec{S}_1)^i r^j - 8 \frac{\vec{r} \cdot \vec{v}_1}{r^2} (\vec{r} \times \vec{S}_1)^i r^j \right] \mathcal{B}_{ij} \\
A_{fig.12Bb} &= 2i \frac{m_1 m_2}{m_{Pl}^4 \Lambda_-^6} \int_{\mathbf{p}, \mathbf{k}} \frac{e^{i\vec{p}\cdot\vec{r}} (\vec{p} - \vec{k}) \cdot \vec{v}_1}{p^2 (p-k)^2 k^2} \\
&\quad \times \left[ \vec{k} \cdot (\vec{p} - \vec{k}) p^i p^j k^m (p-k)^n + \vec{p} \cdot (\vec{p} - \vec{k}) k^i k^j p^m (p-k)^n \right] S_{1mn} \mathcal{B}_{ij} \\
&= 576 \frac{G_N^2 m_1 m_2}{r^2 (\Lambda_- r)^6} \left[ 2 \frac{\vec{r} \cdot \vec{v}_1}{r^2} (\vec{r} \times \vec{S}_1)^i r^j - 2 (\vec{v}_1 \times \vec{S}_1)^i r^j + 7 n^i n^j (\vec{r} \times \vec{v}_1) \cdot \vec{S}_1 \right] \mathcal{B}_{ij}, \\
A_{fig.13a} &= i \frac{m_2^2}{4 m_{Pl}^4 \Lambda_-^6} \int_{\mathbf{p}, \mathbf{k}} \frac{e^{i\vec{p}\cdot\vec{r}} p^k}{p^2 (p-k)^2 k^2} \left\{ 2 \left[ \vec{k} \cdot (\vec{p} - \vec{k}) \right]^2 (p^2 v_1^i \delta^{jl} - v_1^i p^j p^l - \delta^{ik} p^j (\vec{p} \cdot v_1)) \right. \\
&\quad \left. + (p-k)^i (p-k)^j p^k k^l \left( p^2 (\vec{k} \cdot \vec{v}_1) - (\vec{p} \cdot \vec{k}) (\vec{p} \cdot \vec{v}_1) \right) \right\} S_{1kl} \mathcal{B}_{ij} \\
&= 48 \frac{G_N^2 m_2^2}{r^2 (\Lambda_- r)^6} \left[ 33 (\vec{r} \times \vec{S}_1)^i v_1^j - 66 \frac{\vec{r} \cdot \vec{v}_1}{r^2} (\vec{r} \times \vec{S}_1)^i r^j + 5 n^i n^j (\vec{r} \times \vec{v}_1) \cdot \vec{S}_1 \right. \\
&\quad \left. + 7 (\vec{v}_1 \times \vec{S}_1)^i r^j \right] \mathcal{B}_{ij}, \\
A_{fig.13b} &= i \frac{m_2^2}{2 m_{Pl}^4 \Lambda_-^6} \int_{\mathbf{p}, \mathbf{k}} \frac{e^{i\vec{p}\cdot\vec{r}}}{p^2 (p-k)^2 k^2} \\
&\quad \left\{ p^i p^j \left[ \vec{k} \cdot (\vec{p} - \vec{k}) \right]^2 + 2 k^i k^j \left[ \vec{p} \cdot (\vec{p} - \vec{k}) \right]^2 \right\} (v_{1k} p_l S_1^{kl} - p_i S_1^{i0}) \mathcal{B}_{ij} \\
&\quad i 1344 (1 + \kappa) \frac{G_N^2 m_2^2}{r^2 (\Lambda_- r)^6} \left[ 4 n^i n^j (\vec{r} \times \vec{v}_1) \cdot \vec{S}_1 - (\vec{v}_1 \times \vec{S}_1)^i r^j \right] \mathcal{B}_{ij}. \\
A_{fig.13c} &= 384 \frac{G_N^2 m_2^2}{r^2 (\Lambda_- r)^6} \left[ -7 (\vec{r} \times \vec{S}_1)^i v_2^j + 32 \frac{\vec{r} \cdot \vec{v}_2}{r^2} (\vec{r} \times \vec{S}_1)^i r^j + 40 n^i n^j (\vec{r} \times \vec{v}_2) \cdot \vec{S}_1 \right. \\
&\quad \left. - 14 (\vec{v}_2 \times \vec{S}_1)^i r^j \right] \mathcal{B}_{ij}, \\
A_{fig.13d} &= i \frac{m_1 m_2}{m_{Pl}^4 \Lambda_-^6} \int_{\mathbf{p}, \mathbf{k}} \frac{e^{i\vec{p}\cdot\vec{r}}}{p^2 (p-k)^2 k^2} \\
&\quad \left\{ (\vec{p} \cdot \vec{k})^2 (p-k)^k \left[ (\vec{p} - \vec{k})^2 v_1^i \delta^{jl} - v_1^i (p-k)^j (p-k)^l - \delta^{jl} (p-k)^i (\vec{p} - \vec{k}) \cdot \vec{v}_1 \right] \right. \\
&\quad \left. + \frac{p^k k^l}{4} \left[ p^i p^j \left[ \vec{k} \cdot \vec{v}_1 (p-k)^2 - (\vec{p} - \vec{k}) \cdot \vec{v}_1 \vec{k} \cdot (\vec{p} - \vec{k}) \right] \right. \right. \\
&\quad \left. \left. + k^i k^j \left[ (\vec{p} - \vec{k}) \cdot \vec{v}_1 \vec{p} \cdot (\vec{p} - \vec{k}) \right] - (p-k)^2 (\vec{p} \cdot \vec{v}_1) \right] \right. \\
&\quad \left. - k^i k^j p^2 (p-k)^2 (p-k)^k v_1^l \right\} S_{1kl} \mathcal{B}_{ij} \\
&= i 24 \frac{G_N^2 m_1 m_2}{r^2 (\Lambda_- r)^6} \left[ 16 (\vec{r} \times \vec{S}_1)^i v_1^j - 74 \frac{\vec{r} \cdot \vec{v}_1}{r^2} (\vec{r} \times \vec{S}_1)^i r^j + 21 (\vec{r} \times \vec{v}_1) \cdot \vec{S}_1 n^i n^j + \right. \\
&\quad \left. + 10 (\vec{v}_1 \times \vec{S}_1)^i r^j \right] \mathcal{B}_{ij},
\end{aligned} \tag{C6}$$

$$\begin{aligned}
A_{fig.13e} &= i \frac{m_2^2}{m_{Pl}^4 \Lambda_-^6} \int_{\mathbf{p}, \mathbf{k}} \frac{e^{i\vec{p}\cdot\vec{r}}}{p^2 (p-k)^2 k^2} \\
&\quad \left\{ (p-k)^i (p-k)^j (\vec{k} \cdot \vec{p})^2 + p^i p^j (\vec{k} \cdot (\vec{p} - \vec{k}))^2 + k^i k^j (\vec{p} \cdot (\vec{p} - \vec{k})) \right\} \\
&\quad \times \left( v_1^k (p-k)^l S_1^{kl} + (p-k)^k S_1^{0k} \right) \mathcal{B}_{ij} \\
&= 1344 (1 + \kappa) \frac{G_N m_1 m_2}{r^2 (\Lambda_- r)^6} \left[ 4n^i n^j (\vec{r} \times \vec{v}_1) \cdot \vec{S}_1 + (\vec{S}_1 \times \vec{v}_1)^i r^j \right] \mathcal{B}_{ij}, \\
A_{fig.13f} &= 384 \frac{G_N^2 m_1 m_2}{r^2 (\Lambda_- r)^6} \left[ 3 (\vec{r} \times \vec{S}_1)^i v_1^j - 6 \frac{\vec{r} \cdot \vec{v}_1}{r^2} (\vec{r} \times \vec{S}_1)^i r^j + 5n^i n^j (\vec{r} \times \vec{v}_1) \cdot \vec{S}_1 \right. \\
&\quad \left. - 2 (\vec{v}_1 \times \vec{S}_1)^i r^j \right] \mathcal{B}_{ij} \\
A_{fig.13g} &= 768 \frac{G_N^2 m_1 m_2}{r^2 (\Lambda_- r)^6} \left[ -3 (\vec{r} \times \vec{S}_1)^i v_2^j + 18 \frac{\vec{r} \cdot \vec{v}_2}{r^2} (\vec{r} \times \vec{S}_1)^i r^j + 23n^i n^j (\vec{r} \times \vec{v}_2) \cdot \vec{S}_1 \right. \\
&\quad \left. - 14 (\vec{v}_2 \times \vec{S}_1)^i r^j \right] \mathcal{B}_{ij}.
\end{aligned}$$

Expression of amplitudes before momentum integration relative to diagrams in fig. 13c,f,g are very length and have not been reported here.



c.  $\tilde{C}^2$

The three diagrams in fig.15 give the amplitudes

$$\begin{aligned}
A_{fig.15a} &= \frac{16m_2^2}{m_{Pl}^4 \tilde{\Lambda}^6} \int_{\mathbf{p}, \mathbf{k}} \frac{e^{i\vec{p}\cdot\vec{r}}}{p^2 (p-k)^2 k^2} \left\{ \left[ (\vec{p}-\vec{k}) \cdot \vec{k} \right] p^i p^k \delta^{lu} (p-k)^n v_2^r \right. \\
&\quad \left. - (\vec{p} \cdot \vec{k}) (p-k)^i (p-k)^k v_2^l k^n \delta^{ru} \right\} k^m p^s S_{1su} \epsilon_{jkl} \epsilon_{mnr} R_{0i0j} \\
&= i1536 \frac{G_N^2 m_2^2}{\tilde{\Lambda}^6 r^8} \left\{ 16n^i n^j \left[ \vec{S}_1 \cdot (\vec{r} \times \vec{v}_2) \right] - 16n^i (\hat{n} \cdot \vec{v}_2) \left( \vec{S}_1 \times \vec{r} \right)^j \right. \\
&\quad \left. + 6r^i \left( \vec{S}_1 \times \vec{v}_2 \right)^j + 5v_2^i \left( \vec{S}_1 \times r \right)^j \right\} R_{0i0j}, \\
A_{fig.15b} &= \frac{m_1 m_2}{m_{Pl}^4 \tilde{\Lambda}^6} \int_{\mathbf{p}, \mathbf{k}} \frac{e^{i\vec{p}\cdot\vec{r}}}{p^2 (p-k)^2 k^2} \left\{ (\vec{p} \cdot \vec{k}) (p-k)^i (p-k)^k \delta^{lu} k^n v_1^r + \right. \\
&\quad \left. \left[ \vec{p} \cdot (\vec{p}-\vec{k}) \right] k^i k^k v_1^l (p-k)^n \delta^{ru} \right\} p^m (p-k)^s S_{1su} \epsilon_{jkl} \epsilon_{mnr} R_{0i0j} \\
&= -i768 \frac{G_N^2 m_1 m_2}{r^2 (\tilde{\Lambda} r)^6} \left\{ 11n^i n^j \left[ \vec{S}_1 \cdot (\vec{r} \times \vec{v}_1) \right] - 6n^i (\hat{n} \cdot \vec{v}_1) \left( \vec{S}_1 \times \vec{r} \right)^j \right. \\
&\quad \left. + 2r^i \left( \vec{S}_1 \times \vec{v}_1 \right)^j + 3v_1^i \left( \vec{S}_1 \times \vec{r} \right)^j \right\} R_{0i0j}, \\
A_{fig.15c} &= \frac{m_1 m_2}{m_{Pl}^4 \tilde{\Lambda}^6} \int_{\mathbf{p}, \mathbf{k}} \frac{e^{i\vec{p}\cdot\vec{r}}}{p^2 (p-k)^2 k^2} \left\{ p^i p^k v_2^l \delta^{\mu u} k^n (p-k)^r \left[ \vec{k} \cdot (\vec{p}-\vec{k}) \right] \right. \\
&\quad \left. (p-k)^i (p-k)^k \delta^{lu} v_2^m k^n p^r \right\} (p-k)^s S_{1su} \epsilon_{jkl} \epsilon_{mnr} R_{0i0j} \\
&= i1536 \frac{G_N^2 m_1 m_2}{r^2 (\tilde{\Lambda} r)^6} \left\{ 47n^i n^j \left[ \vec{S}_1 \cdot (\vec{r} \times \vec{v}_2) \right] - 42n^i (\hat{n} \cdot \vec{v}_2) \left( \vec{S}_1 \times \vec{r} \right)^j \right. \\
&\quad \left. + 32r^i \left( \vec{S}_1 \times \vec{v}_2 \right) - 6v_2^i \left( \vec{S}_1 \times \vec{r} \right)^j \right\} R_{0i0j},
\end{aligned} \tag{C7}$$

and their sum gives eq. (65).

The two diagrams in fig.16 give the amplitudes

$$\begin{aligned}
A_{fig.16a} &= -\frac{4m_2^2}{m_{Pl}^4 \tilde{\Lambda}^6} \int_{\mathbf{p}, \mathbf{k}} \frac{e^{i\vec{p}\cdot\vec{r}} (\vec{p} \cdot \vec{k})}{p^2 k^2 (p-k)^2} (p-k)^i (p-k)^j k^m p^n p^s S_1^{sr} \epsilon_{mnr} \mathcal{B}_{ij} \\
&= i768 \frac{G_N^2 m_2^2}{\tilde{\Lambda}^6 r^8} \left[ -5S_1^i r^j + 8n^i n^j \left( \vec{S}_1 \cdot \vec{r} \right) \right] \mathcal{B}_{ij} \\
A_{fig.16b} &= -\frac{4m_1 m_2}{m_{Pl}^4 \tilde{\Lambda}^6} \int_{\mathbf{p}, \mathbf{k}} \frac{e^{i\vec{p}\cdot\vec{r}}}{p^2 (p-k)^2 k^2} \left\{ \left[ (\vec{p}-\vec{k}) \cdot \vec{k} \right] p^i p^j k^m p^n \right. \\
&\quad \left. - \left[ (\vec{p}-\vec{k}) \cdot \vec{p} \right] k^i k^j p^m k^n \right\} (p-k)^s S_{1sr} \epsilon_{mnr} \mathcal{B}_{ij} \\
&= i2304 \frac{G_N m_1 m_2}{\tilde{\Lambda}^6 r^8} \left[ -S_1^i r^j + 6n^i n^j \left( \vec{S}_1 \cdot \vec{r} \right) \right] \mathcal{B}_{ij},
\end{aligned} \tag{C8}$$

which allow the derivation of eq. (66).

- [2] R. Abbott et al. (LIGO Scientific, Virgo) (2020), 2010.14527.
- [3] J. Aasi et al. (LIGO Scientific), *Class. Quant. Grav.* **32**, 074001 (2015), 1411.4547.
- [4] F. Acernese et al. (VIRGO), *Class. Quant. Grav.* **32**, 024001 (2015), 1408.3978.
- [5] B. Allen, W. G. Anderson, P. R. Brady, D. A. Brown, and J. D. E. Creighton, *Phys. Rev. D* **85**, 122006 (2012), gr-qc/0509116.
- [6] S. Endlich, V. Gorbenko, J. Huang, and L. Senatore, *JHEP* **09**, 122 (2017), 1704.01590.
- [7] W. D. Goldberger and I. Z. Rothstein, *Phys. Rev. D* **73**, 104029 (2006), hep-th/0409156.
- [8] R. A. Porto and I. Z. Rothstein, *Phys. Rev. Lett.* **97**, 021101 (2006), gr-qc/0604099.
- [9] R. A. Porto, *Phys. Rept.* **633**, 1 (2016), 1601.04914.
- [10] M. Levi and J. Steinhoff, *JHEP* **09**, 219 (2015), 1501.04956.
- [11] X. O. Camanho, J. D. Edelstein, J. Maldacena, and A. Zhiboedov, *JHEP* **02**, 020 (2016), 1407.5597.
- [12] B. Kol and M. Smolkin, *Class. Quant. Grav.* **25**, 145011 (2008), 0712.4116.
- [13] S. Foffa and R. Sturani, *Phys. Rev. D* **84**, 044031 (2011), 1104.1122.
- [14] S. Foffa and R. Sturani, *Phys. Rev. D* **87**, 064011 (2013), 1206.7087.
- [15] K. S. Thorne, *Rev. Mod. Phys.* **52**, 299 (1980).
- [16] A. J. Hanson and T. Regge, *Annals Phys.* **87**, 498 (1974).
- [17] R. A. Porto, *Phys. Rev. D* **73**, 104031 (2006), gr-qc/0511061.
- [18] M. Mathisson, *Acta Phys. Polon.* **6**, 163 (1937).
- [19] A. Papapetrou, *Proc. Roy. Soc. Lond. A* **A209**, 248 (1951).
- [20] W. Dixon, *Proc. Roy. Soc. Lond. A* **A314**, 499 (1970).
- [21] H. Goldstein, *Classical Mechanics* (Addison-Wesley, 2002).
- [22] B. Barker and R. O'Connell, *Phys. Rev. D* **12**, 329 (1975).
- [23] S. Foffa and R. Sturani, *Class. Quant. Grav.* **31**, 043001 (2014), 1309.3474.
- [24] B. Barker and R. O'Connell, *Phys. Rev. D* **2**, 1428 (1970).
- [25] K. S. Thorne and J. B. Hartle, *Phys. Rev. D* **31**, 1815 (1985).
- [26] E. Poisson and M. Sasaki, *Phys. Rev. D* **51**, 5753 (1995), gr-qc/9412027.
- [27] L. E. Kidder, C. M. Will, and A. G. Wiseman, *Phys. Rev. D* **47**, R4183 (1993), gr-qc/9211025.
- [28] L. E. Kidder, *Phys. Rev. D* **52**, 821 (1995), gr-qc/9506022.
- [29] B. Abbott et al. (LIGO Scientific, Virgo), *Phys. Rev. D* **100**, 104036 (2019), 1903.04467.
- [30] R. Abbott et al. (LIGO Scientific, Virgo) (2020), 2010.14529.

- [31] N. Sennett, R. Brito, A. Buonanno, V. Gorbenko, and L. Senatore, *Phys. Rev. D* **102**, 044056 (2020), 1912.09917.
- [32] V. Cardoso, M. Kimura, A. Maselli, and L. Senatore, *Phys. Rev. Lett.* **121**, 251105 (2018), 1808.08962.
- [33] R. P. Breton, V. M. Kaspi, M. Kramer, M. A. McLaughlin, M. Lyutikov, S. M. Ransom, I. H. Stairs, R. D. Ferdman, F. Camilo, and A. Possenti, *Science* **321**, 104 (2008), 0807.2644.
- [34] B. Perera et al., *Astrophys. J.* **721**, 1193 (2010), 1008.1097.
- [35] D. Perrodin and A. Sesana, *Astrophys. Space Sci. Libr.* **457**, 95 (2018), 1709.02816.
- [36] C. W. F. Everitt, D. B. DeBra, B. W. Parkinson, J. P. Turneare, J. W. Conklin, M. I. Heifetz, G. M. Keiser, A. S. Silbergleit, T. Holmes, J. Kolodziejczak, et al., *Phys. Rev. Lett.* **106**, 221101 (2011), 1105.3456, URL <https://link.aps.org/doi/10.1103/PhysRevLett.106.221101>.
- [37] E. Racine, A. Buonanno, and L. E. Kidder, *Phys. Rev. D* **80**, 044010 (2009), 0812.4413.
- [38] A. Ross, *Phys. Rev. D* **85**, 125033 (2012), 1202.4750.